

# Dynamic Processes in Ionic Glasses

C. A. ANGELL

Department of Chemistry, Arizona State University, Tempe, Arizona 85287-1604

Received November 6, 1989 (Revised Manuscript Received February 14, 1990)

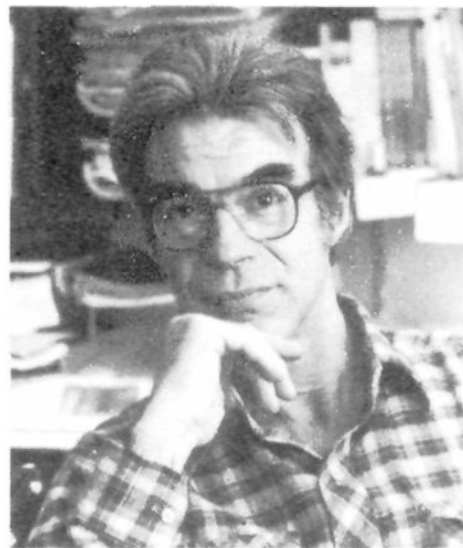
## Contents

I. Introduction	523
II. Vitrification, Primary and Secondary Relaxation Processes in Amorphous Systems, and Scope of the Review	524
III. Relaxation Functions, Complex Moduli, and Constant $T$ vs Constant $f$ Experiments	527
IV. Dependence of Glassy Dynamics on Thermal History	529
V. Comparison of Electrical and Mechanical Relaxation Spectra	530
VI. Comparison of Electrical and Nuclear Magnetic Relaxation Data	532
VII. Correlation of Relaxation Spectra with Decoupling Index and Structure	534
VIII. Connections between Relaxational and Vibrational Responses	536
IX. Omissions	539
X. Conclusions	540
XI. Acknowledgments	540
XII. References	540

## I. Introduction

The field of dynamic processes occurring within the glassy state of matter is too broad to be dealt with in a single article. There is, for instance, an enormous literature on the subject of tunneling modes (two-level systems) which leads glassy solids systematically to violate the Debye  $T^3$  law for the low-temperature heat capacity of solids. To this must be added a relevant and rapidly growing literature on the "hole-burning" phenomenon. There is an even larger literature on secondary, tertiary, and quaternary relaxations in polymeric glasses, the understanding of which is of great importance for many technological applications of polymeric materials. Both of these research fields lie outside this reviewer's area of interest and competence. We will, accordingly, restrict our attention to a subsection of the broader subject and focus most of our attention on the phenomenology of dynamic processes in ionic glasses at temperatures well above 0 K. However, we will give an initial minireview section (section II) to locating the problem area that we will review within the broader subject.

While the author knows of no previous review that attempts to cover the same range of subject matter from the same approach, there are a number of important articles, which review in greater depth than we can here, various individual aspects of the subject. We assemble these references, several of which appear in a current thematic issue of *Materials Chemistry and Physics* (Vol. 23, nos. 1/2), in ref 1a. We will, however, refer to the most relevant articles individually in the text.



C. A. Angell was born in Canberra, Australia, in 1933, and studied to the M.Sc. level at the University of Melbourne. After working on molten salts in the electrochemistry group of J. O'M. Bockris at the University of Pennsylvania for 2 years, he became the Stanley Elmore Fellow at the Imperial College of Science, London. While there, he obtained a Ph.D. as a student of J. W. Tomlinson, winning the Armstrong medal for graduate research at Imperial College for 1959-1961. He then returned to Melbourne, but after 2 years as a lecturer in chemical metallurgy he came back to the United States as a Research Associate with D. M. Gruen at Argonne National Laboratory. In 1966 he joined Purdue University as an Assistant Professor, becoming full Professor in 1971. He has profited from one-semester sabbatical leaves in Holland (University of Amsterdam) in 1970, Australia (The National University) in 1975, and France (Inst. Laue Langevin in 1979 and Ecole de Physique et Chemie, Paris, in 1983). His research interests spread from water through aqueous and polymeric solutions to molten salts, glassy solid electrolytes, and glassy solids in general, with particular emphasis on the motion of particles and the time scales on which stresses imposed on liquid and glassy systems are relaxed. Recently he has become involved in geochemistry via his computer simulation and laboratory studies of liquid silicates and in the properties of liquids at negative pressures. In 1989 he accepted a position in the Department of Chemistry, Arizona State University, where he is pursuing several new lines of research in collaboration with ASU scientists specialized in high-pressure and microscience techniques.

Almost all liquids, when cooled either fast enough or in small enough sample sizes, will fail to find the channel in phase space leading to the crystalline state.<sup>2</sup> Then as the particle kinetic energies become too small to permit diffusion, the viscosity diverges and the system becomes locked into the amorphous state as a glass. Liquids as simple and familiar as toluene are easily vitrified in bulk, and even benzene may be vitrified on normal time scales when in the form of 2-300-Å droplets in microemulsions.<sup>3,4</sup>

To many workers, the process of slowing down of the viscous modes, which is currently the subject of a great deal of experimental and theoretical activity,<sup>5</sup> is one aspect of *glassy* dynamics, and the absence of a detailed discussion of the subject in this article may seem to be a serious if not glaring omission. However, while slow-

ing down in liquids is an area of great interest to this author, it is his view that the behavior of an amorphous phase in *metastable equilibrium* (i.e., when the sample under study is in internal equilibrium both before and after it is probed by the experimentalist) belongs to the field of *liquid state*, not *glassy state*, studies. Thus the many studies on dielectric relaxation, ultrasonic and hypersonic relaxation, NMR, and ac heat capacity in viscous liquids<sup>5</sup> will be excluded from the review. Rather, the review will focus on those modes of motion that remain active in the temperature (or pressure) regime that lies below (or above) the glass transition temperature (or pressure), i.e., in the state in which the majority of the particles in the system are "frozen" into a fixed configuration. The actual configuration is, of course, not unique, and much of the behavior that we will review will in fact be determined by the manner in which the system passes initially into the glassy (i.e., nonergodic) state. Let us thus first examine the process of vitrification.

## II. Vitrification, Primary and Secondary Relaxation Processes in Amorphous Systems, and Scope of the Review

Vitrification occurs because of the crossing of the intrinsic liquid relaxation time scale and the external, experimentalist-controlled, observation time scale. Let us consider cooling as a series of stepwise decreases in temperature followed by short (isothermal) equilibration periods. Initially, when the liquid relaxation time is very short, the equilibration time  $\Delta t$  is quite sufficient for the system to explore its full configuration space before the next drop in temperature  $\Delta T$  occurs. However, because the relaxation time  $\tau$  is increasing with decreasing temperature (at a rate that depends on the liquid "fragility"; see below) at some point during the cooling, a temperature must be reached at which the liquid will not be fully equilibrated (ergodic) before the next  $\Delta T$  decrease in temperature occurs. Since, after this next  $\Delta T$ , the mismatch of  $\tau$  and  $\Delta t$  will be worse, so the degree of equilibration achieved in the next (and in each subsequent)  $\Delta T$ , will rapidly diminish—and will soon become undetectable (see Figure 5 of ref 6). At this point the liquid configuration (its "structure") has become fixed except for minor adjustments due to decreasing vibrational anharmonicity and to more or less localized, low energy barrier, configurational adjustments—the so-called secondary relaxations on which this review will be focused. The substance is said to be "vitreous" and textbooks describe it as a "frozen liquid". As we shall see, it is in fact alive with irreversible motions of different types. These motions can be so free as to lead, in some cases, to glassy materials that exhibit ambient temperature electrical conductivities not much below that of battery acid and, in others, to glasses with the ability to absorb large amounts of mechanical energy on very short time scales—e.g., in high impact strength polymers.

The temperature range over which the liquid passes from the fully ergodic metastable state into the glassy state (called the "glass transformation range") is effectively the temperature change needed to change the relaxation time by about 2 orders of magnitude across the experimental cooling time scale.<sup>6-8</sup> This temperature range is different for different systems and also for

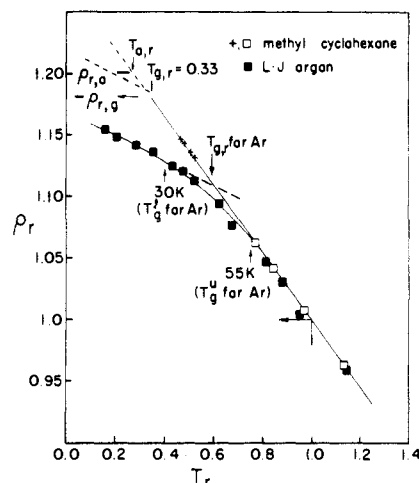
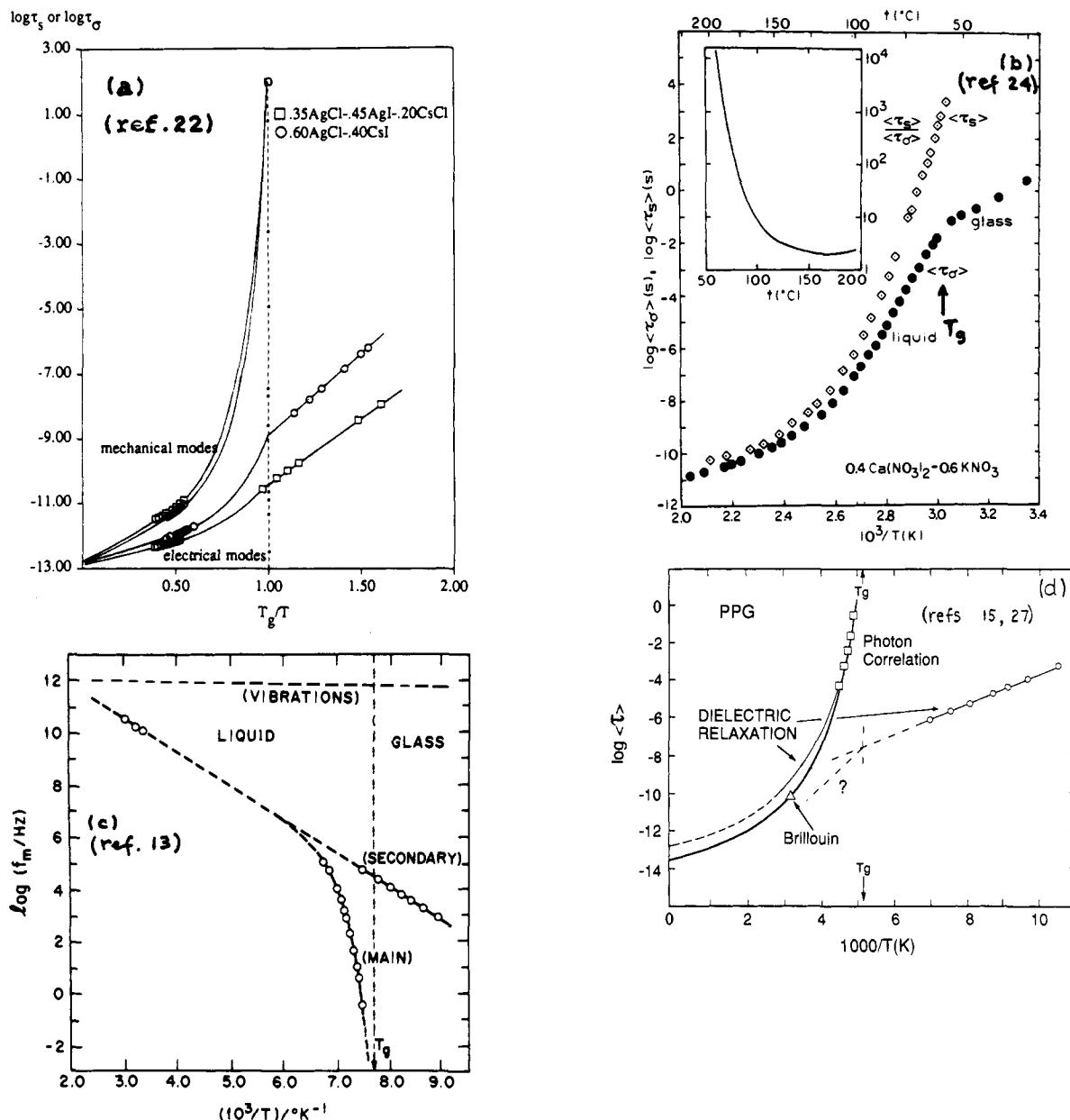


Figure 1. Dependence of glass density on quenching rate  $q$  using reduced variables. For methylcyclohexane  $q = -10$  K/min, while for LJ argon  $q = -10^{12}$  K/min (by computer simulation). Corresponding states are states of equal diffusivities,  $D = 10^{-5}$  cm<sup>2</sup> s<sup>-1</sup>. Reprinted from ref 10; copyright 1981 New York Academy of Sciences.

different cooling or compression rates. It is smallest for systems that have very large temperature dependences of their relaxation times in the region where equilibrium is being lost and that also have only narrow distributions of relaxation times. Since distributions tend to be narrowed under conditions where the temperature dependence is smaller (e.g., (i) "strong", as opposed to "fragile",<sup>9</sup> liquids being vitrified on normal time scales or (ii) fragile liquids being vitrified on short, as opposed to long, time scales), these effects are somewhat related. However, it is not of great importance for the purpose of this review that the relationships be analyzed. It is important, however, to emphasize the differences in density of the vitrified material that may result from differences in the rate of cooling through the glass transformation range, since the packing in the glass may be expected to play an important role in the dynamics of processes occurring in the glassy structure.

Figure 1 shows, in reduced units, an extreme case<sup>10</sup> where we compare the densities of two van der Waals glasses, one (methylcyclohexane) produced by ordinary laboratory time scale cooling and the other (Lennard-Jones argon) produced by the very fast quenching procedure employed (faute de mieux) in molecular dynamics computer simulation "experiments". The corresponding states used in the reduction (which are explained in the original publication<sup>6,10</sup>) were chosen as the states exhibiting liquid diffusion coefficients of  $10^{-5}$  cm<sup>2</sup> s<sup>-1</sup>. Figure 1 (from ref 10) shows that the slower cooled system achieves a density approximately 5% greater than that of the hyperquenched system. It can readily be imagined that the residual dynamics in the glassy state can be generally affected by such a difference in packing densities.

The presence of residual looseness in glassy phases implies that the system should exhibit an anelastic response to mechanical stresses. This is because the local displacement of particles at loose spots in the overall jammed structure can serve to relax the applied stress, in a reversible manner. Certainly, such elastic responses (which were predicted to be a universal feature of the glassy state in a classic paper by Goldstein<sup>11</sup>) are very generally (though not universally) observed.<sup>12</sup> If the



**Figure 2.** (a) Comparison of average shear and electrical relaxation times, reflecting slow and fast processes for liquid and glassy states of ionic 3AgCl-2CsI solution (reprinted from ref 22; copyright 1988 American Chemical Society). (b) Comparison of average shear and electrical relaxation times, reflecting slow and fast processes for liquid and glassy 3KNO<sub>3</sub>-2Ca(NO<sub>3</sub>)<sub>2</sub> solution (reprinted from ref 24a; copyright 1974 American Chemical Society). (c) Comparison of most probable dielectric relaxation times for slow (primary) and fast (secondary) relaxation processes in *cis*-decalin + 17.2% chlorobenzene solution.<sup>15</sup> Dashed line shows approximate behavior of the average relaxation time for the secondary process. (d) Comparison of most probable dielectric relaxation times for slow (primary) dielectric and mechanical relaxation times<sup>27</sup> and fast (secondary) dielectric relaxation times for poly(propylene oxide).<sup>14</sup> (Secondary relaxation data taken from ref 15).

local displacement involves a change of dipole moment, such relaxations can also be detected by electrical field relaxation or dielectric relaxation methods. In fact, the majority of studies of such localized relaxation processes in simple molecular glasses have been made by using dielectric relaxation techniques.<sup>12,14-16</sup>

The existence of anelastic processes detectable by frequency-dependent or time-dependent techniques implies the presence of at least one additional time scale in the dynamics of amorphous systems—a time scale that is short with respect to that of the viscoelastic process that leads to the glass transition. It is important in introducing this subject that the relation of these time scales be established. This is particularly so since the existence of a shorter time scale is a clear prediction of one of the most activity researched theoretical ap-

proaches to the slowing-down problem in liquids, viz., the mode coupling theory<sup>17-20</sup> (which is developed in elegant detail by Goetze in a recent lecture series<sup>20</sup>).

It seems that there are at least two distinct classes of dynamic processes residual in glasses to be considered: (i) short-time relaxation processes due to decoupled delocalized motion of a minority species in ionic glasses, and (ii) short-time processes due to strictly *localized* motions that are predominant in organic and polymer glasses but are also present in inorganic glasses, including the ionic cases. Metallic glasses may be close in nature to the ionic case insofar as a fraction of the particles may retain considerable long-range mobility in the frozen vitreous state.<sup>21</sup>

We depict the relationship of long- and short-time processes for four cases in Figure 2. In Figure 2a, which

shows relaxation time data for the system 3AgCl-2CsI (and a related composition) in both liquid and vitreous states,<sup>22</sup> the Ag<sup>+</sup> ion motions are highly decoupled from the remainder. Because Ag<sup>+</sup> is a charge carrier, the fast relaxation process is easily monitored via the electrical relaxation time  $\langle\tau_\sigma\rangle$ .  $\langle\tau_\sigma\rangle$  here is a Maxwell-like relaxation time defined by the relation<sup>23,24</sup>

$$(\sigma_{dc})^{-1} = M_\infty \langle\tau_\sigma\rangle / e_0 \quad (1)$$

where the electrical modulus,  $M_\infty$ ,<sup>23</sup> is the inverse of the dielectric constant measured at frequencies much higher than  $(2\pi\langle\tau_\sigma\rangle)^{-1}$ ,  $e_0$  is the permittivity of free space ( $=8.85 \times 10^{-14}$  F cm<sup>-1</sup>), and  $\sigma_{dc}$  is the dc electrical conductivity.  $\tau_\sigma$  is written as an average value because, when studied as a function of frequency, the electrical relaxation process is found to be nonexponential in nature; i.e., it cannot be characterized by a single time constant (see below). The important observations in Figure 2a are (a) that the short-time process is always distinguishable in time scale ( $\langle\tau_\sigma\rangle$ ) from the longer, viscoelastic (or structural relaxation) process ( $\langle\tau_s\rangle$ ) and (b) the time scale ratio  $\langle\tau_s\rangle/\langle\tau_\sigma\rangle$ , which was first examined by Moynihan and colleagues<sup>24</sup> and is now known as the *decoupling index*,  $R_\tau$ ,<sup>25</sup> increases continuously with decreasing temperature. In this case  $R_\tau$  reaches very large values,  $\sim 10^{12}$ , at the glass transition temperature  $T_g$ , though the system is exceptional (it is characteristic of the so-called "superionic" glasses which have liquid-like conductivities ( $\sigma \approx 10^{-2}$   $\Omega^{-1}$  cm<sup>-1</sup>) at their glass transition temperature<sup>25,26</sup>). More generally, as shown for the much-studied molten nitrate system in Figure 2b, the electrical relaxation process in ionic systems is similar in time scale to the viscoelastic process when the temperature is high relative to  $T_g$  but progressively decouples from it as  $T$  falls below  $\sim 1.3T_g$ .<sup>24</sup> Both show non-Arrhenius behavior initially but the faster process frequently returns to Arrhenius behavior well before  $T_g$  is reached. At  $T_g$  the plot abruptly changes slope as the glassy state is entered and the overall structure freezes. The temperature dependence of the dc conductivity usually remains strictly Arrhenius in the glassy state though exceptions exist (see below). At lower temperatures, where the relaxation process occurs on time scales accessible to regular admittance bridges, more detailed studies of the process may be made via variable-frequency studies. These will be discussed in the body of the review to follow.

To contrast with the ionic glass formers, Figure 2c shows the behavior observed in simple *molecular* liquids, while Figure 2d shows data for a chain polymer system.<sup>14,27</sup> In the case of molecular glasses, most information on the faster process (usually called the *secondary* relaxation) has been acquired by dielectric relaxation studies.<sup>12-15</sup> While the overall appearance—Arrhenius behavior of the faster process below  $T_g$  with a tendency for it to join the primary relaxation in the liquid state—is similar to that seen in Figure 2a,b, there are distinct differences. The main difference, if we accept the data and extrapolations of the reporting authors, is that the secondary relaxations in the molecular systems are insensitive to the structural arrest occurring at the glass transition. An insensitivity to structural arrest implies that the frequency of maximum loss would not change on annealing (as the liquid relaxes to lower volumes), and Johari and

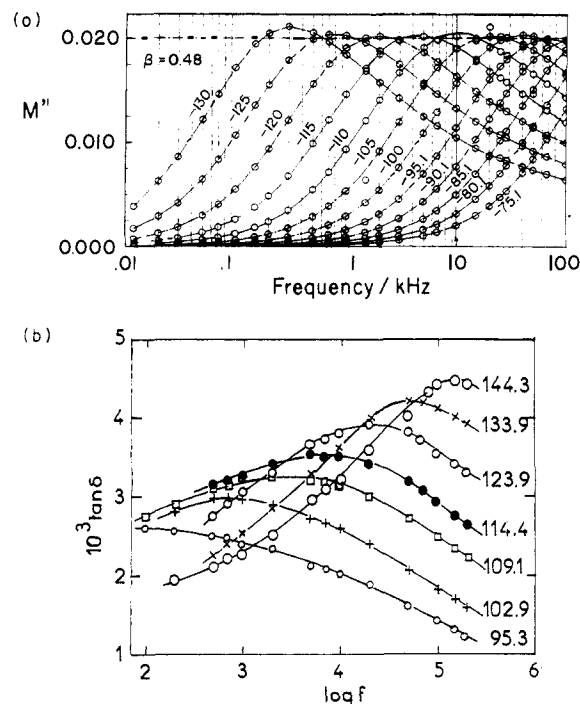


**Figure 3.** Contrast between secondary electrical relaxation spectra in (a) ionic 3AgI-2Ag<sub>2</sub>B<sub>4</sub>O<sub>7</sub><sup>38</sup> and (b) molecular poly(propylene oxide)<sup>15</sup> systems. In the ionic case all relaxation spectra have identical shapes, well described by a KWW function (eq 1) with  $\beta = 0.55$ . In the molecular cases the best description is open to debate (see text).

co-workers have provided evidence that this is the case for some molecular,<sup>13</sup> polymeric,<sup>13</sup> and covalent glasses.<sup>28</sup>

The contrast between the two secondary relaxations in Figure 2c,d illustrates a point of some dispute among workers in this area. The issue in dispute is whether the secondary process should be viewed as colliding with or merging with the primary process. A difficulty in the path of resolving this issue is raised by another major difference between ionic and nonionic cases—a difference that is not evident in Figure 2. This difference concerns the width and temperature dependence of the secondary relaxations in the two cases. In the ionic cases the width of the electrical relaxation (whether or not considered as a single process<sup>24</sup> or as a combination of conductivity and ion-pair dipolar relaxation processes,<sup>29</sup>) is as narrow as the primary viscoelastic relaxation. In the nonionic cases, however, the relaxation not only is much broader but is usually also strongly temperature dependent. This important distinction, which involves one of the fundamental issues of disordered-phase dynamics (viz., the origin of nonexponential relaxation kinetics), is illustrated in Figure 3.

Figure 3a shows that the "loss spectra", i.e., the out-of-phase, or imaginary, part of the complex electrical modulus discussed below, for the fast ion conducting glass 3AgI-2Ag<sub>2</sub>B<sub>4</sub>O<sub>7</sub> have a temperature-independent shape, in marked contrast with the case of the polymer poly(propylene oxide) (PPO). The rapidly changing shape of the spectra for PPO is typical of the observations for molecular and polymer glasses.<sup>12-14</sup> The rapidly changing shape in these cases means that the average relaxation time will have a different (larger) temperature dependence than the most probable value plotted in Figure 2d and so will show less tendency to intersect the primary relaxation. The broad spectra, the difficulty of separating out the contributions of the

primary process and background losses from those due to the secondary process, and the fact that the total polarization associated with the secondary relaxation decreases with decreasing temperature,<sup>12-14</sup> introduce an ambiguity into the relation between primary and secondary relaxations in the nonionic cases that is not present in the ionic cases. This ambiguity presents a challenge for future workers since it has been forcefully argued<sup>30</sup> that the secondary relaxations in molecular glasses are actually the source and necessary precursor of the primary relaxation which receives most of the theoretical as well as experimental attention.

In any event, Figure 2 now allows us to define the scope of this review in relation to the broader scheme of relaxation dynamics in amorphous systems. Rather than examining in detail all of the phenomena plotted in Figure 2 (not to mention the additional widely researched area of relaxation phenomena found at cryogenic temperatures (the so-called two-level systems)), we will concentrate on the behavior of the subset of processes that may be detected below  $T_g$  in ionic systems like those of Figure 2a,b, i.e., secondary relaxations due to mobile ions in ionic glasses. Many of the systematic aspects of the observations we will discuss will probably be found applicable to the organic systems when the detailed studies necessary to discuss the issues are performed. Many detailed studies of the type we will discuss for ionic systems have in fact *already* been performed on *polymeric* systems. These, however, constitute an entire research field of their own which is complicated by the presence of tertiary and quaternary ( $\gamma$ ,  $\delta$ ) relaxations and which we make no attempt to enter. The interested reader may consult a rather exhaustive review of "relaxation maps" for polymer systems given by Törmälä.<sup>31</sup>

While the scope of our review may seem rather limited, we will, in fact, be examining results of a wide range of experiments covering 18 orders of magnitude in time scale and 1000 K in temperature. From the overview provided, a number of useful unifying patterns, and suggestions for future experimental and theoretical studies, will emerge.

There are three major problem areas to be addressed. They are as follows:

(1) What is the response function for the fast process, and how is it related to perturbing stress on the one hand and to the glass structure on the other?

(2) What determines the value of the average relaxation time for the fast process at some reference temperature, e.g., the glass transition temperature at which slow processes have a common relaxation time ( $\sim 10^2$  s). In other words, what determines the extent of decoupling of fast from slow processes.

(3) How are the fast processes related to the even faster degrees of freedom involved in the vibrational modes of the amorphous phase?

We will deal with these questions in this order but must first provide background material concerning the most appropriate manner of acquiring and presenting the desired information.

### III. Relaxation Functions, Complex Moduli, and Constant $T$ vs Constant $f$ Experiments

Before examining in detail the observations on relaxation processes in ionic glasses, it is necessary to

consider the sort of experiments that are commonly carried out and the manner in which the results are presented.

What is common to all the measurements we will discuss is that a system in an initial state is perturbed by some external force and the response is monitored. What is different is the nature of the perturbing stress and the way the stress is applied and the response observed. While it is conceptually simpler to produce an instantaneous perturbation of the system and monitor its decay in time, this is not the way most experiments in this field are performed. Rather, experiments are conducted in the frequency domain because details of the relaxation kinetics are in most cases more accurately acquired by frequency-domain techniques. Thus we will be considering mostly *electrical* perturbations that are applied sinusoidally at variable frequencies in a constant-temperature experiment and *mechanical* or *magnetic* perturbations that are applied sinusoidally at fixed frequency at varying temperatures. The differences are due to the exigencies of the experiment: it is much simpler to produce a wide range of frequencies in electrical experiments than in mechanical or magnetic (NMR) experiments.

Responses of the system are measured as real and imaginary parts of complex electrical or mechanical moduli

$$M^* = M' + iM'' = \frac{\epsilon'}{\epsilon'^2 + \epsilon''^2} - \frac{i\epsilon''}{\epsilon'^2 + \epsilon''^2} \quad (2)$$

or the corresponding susceptibilities  $\epsilon^*$ , depending on the formalism employed in the analysis. Opinions vary on which formalism is the more appropriate to use for a given set of measurements.<sup>23,29,32,33</sup> It must be remembered, however, that the characteristic relaxation time of a process extracted from a given set of data depends somewhat on the formalism employed in the analysis. The relationship is<sup>1a(i)</sup>

$$\frac{\tau(\text{susceptibility formalism})}{\tau(\text{modulus formalism})} = \frac{\epsilon_0}{\epsilon_\infty} = \frac{M_\infty}{M_0} \quad (3)$$

Comparisons of response times for different processes should therefore always be made for data analyzed by the same formalism. Because the zero-frequency electrical modulus is always zero for electrically conducting systems such as the ionic glasses of this review, we will analyze all data in the modulus formalism. In ordinary circumstances, i.e., when the system reaches a thermodynamic state of polarization as a long-time response to the perturbation, it is preferable to compare different responses in the susceptibility formalism. This avoids the possibility of differences in response times to different perturbations, which result from analysis formalism rather than to real differences at the molecular level.

A typical set of data for an electrical relaxation experiment on ionic glasses is that shown in Figure 4 for  $\text{Na}_2\text{O}\cdot 3\text{SiO}_2$ .<sup>34</sup> The upper portion shows how the real part of the electrical modulus rises from its low-frequency value of zero toward a high-frequency limit, the dispersion region moving to high frequencies as the temperature of the experiment is increased. The lower portion shows the imaginary part of the modulus, which is related to the energy dissipation taking place in the irreversible conduction process. The relaxation process

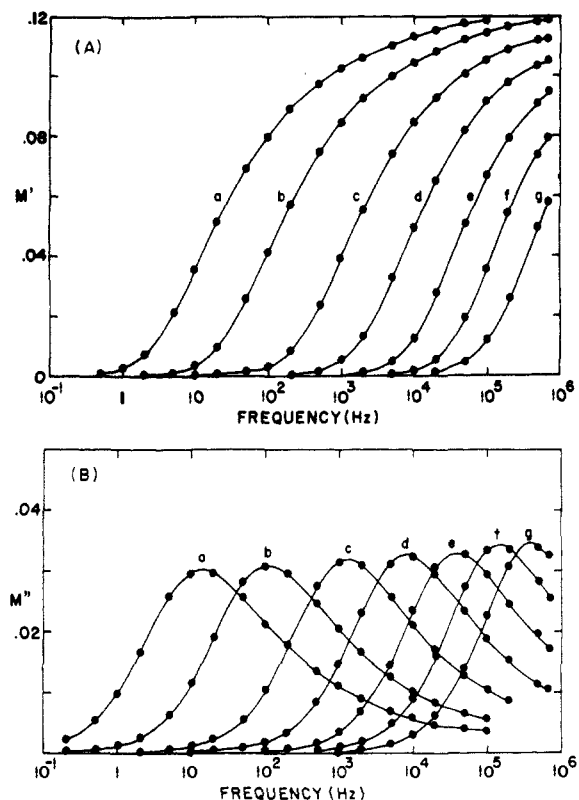


**Figure 4.** Electrical relaxation in a typical ionic glass. (A) Real,  $M'$ , and (B) imaginary,  $M''$ , parts of the complex electrical modulus for  $\text{Na}_2\text{O}-3\text{SiO}_2$  glass over a range of temperatures below  $T_g$ : (a)  $-1$ , (b)  $20.8$ , (c)  $52.3$ , (d)  $81.4$ , (e)  $110.2$ , (f)  $137.3$ , and (g)  $163.4$  °C. The spectra are well fitted by a Williams-Watts function (eq 1) with  $\beta = 0.7$ . Reprinted from ref 34; copyright 1972 American Ceramic Society.

is not exponential,  $e^{-(t/\tau)}$ , since the spectrum is not a Lorentzian. Its skewed shape is well represented, for poorly conducting glasses at least, by the appropriate Laplace transform of the Kohlrausch decay function

$$\phi(t) = e^{-[(t/\tau)^\beta]}, \quad 0 < \beta < 1 \quad (4)$$

(where  $\phi(t)$  is normalized by its value at  $t = 0$ ) as was first recognized for ionic glasses by Moynihan et al.<sup>35</sup> and which has been abundantly documented for these and other systems by Ngai and co-workers<sup>16</sup> (see in particular ref 16b, which gives an exceptionally detailed account of this phenomenology and its relation to primary relaxations). The most probable relaxation time  $\tau_o$  is obtained from the frequency at maximum loss by  $\tau_o = (2\pi f_{\text{max}})^{-1}$ . It is found to vary with temperature according to the Arrhenius law.

Before going any further, we should discuss the recent suggestion of Johari and Pathmanathan<sup>29</sup> that the  $M''$  spectra for ionic glasses are actually a combination of an exponential conductivity relaxation spectrum (a Lorentzian) and an ion-pair dipole relaxation and that the former should be subtracted out before the latter is analyzed. As the authors point out, this is a new application of the idea common to the earlier studies of glasses<sup>32</sup> in which the more common susceptibility formalism<sup>32</sup> was used for data analysis and a dc contribution to the observed dielectric loss was subtracted out before the residual loss was analyzed (as has always been the practice in dielectric relaxation studies). Johari and Pathmanathan show that the  $M''$  spectra can be quantitatively fitted under this assumption using a Kohlrausch-Williams-Watts (KWW) function for the

dielectric component. By contrast, the single KWW function used by earlier authors leaves a high-frequency component of the observed modulus spectrum unaccounted for. The improved fit is, of course, obtained at the expense of introducing additional adjustable parameters, and the procedure should therefore be shown to have predictive value to warrant the loss of simplicity involved in adopting it.

One prediction pointed out in ref 29 was that, at low temperatures, the single spectrum normally seen would be resolved into two if the dipolar and conductivity relaxation processes were distinguished by different activation energies, as would seem reasonable. Conductivity relaxation measurements on insulating glasses are not easy to perform, so this possibility has yet to be fully checked out. At the limit of lightly doped silica, Simmons and Simmons<sup>36</sup> have observed a single-exponential relaxation and, so far, the broadest  $M''$  peak seems to be correlated with the largest conductivities and largest decoupling indexes (see below). The fact that most  $M''$  spectra, for both normal and superionic glasses, have shapes that are almost temperature independent<sup>35,37,38</sup> means that if separate conductivity and dipolar processes do exist, then they mostly involve the same energy barriers (unless variations in  $d\Delta\epsilon/dT$  and  $d\tau/dT$  happen to compensate so as to maintain constant shape). Therefore, until some unambiguous means of demonstrating their separate existence can be found, we will adopt the convenience of treating them as a single coupled process and will seek correlations between the parameters describing the electrical modulus dispersion and loss spectrum and other responses of the same systems to distinguishable stresses, e.g., mechanical and magnetic. We must, however, keep open the possibility that these modulus parameters may, in the future, need to be modified if the case for separating dielectric and conductivity responses becomes compelling.

In the latter respect, particular attention should be drawn to the recent work of Hyde and Tomazawa.<sup>45</sup> These authors use the conventional approach to extract a static dielectric constant, which they interpret as due to alkali diffusion-induced composition changes (as opposed to dipole relaxation) and, using an electrical analogue of Zener's anelasticity theory, relate to the (frozen-in) composition fluctuations associated with nonideal mixing. Indeed, they show rather persuasive correlations of the derived dielectric dispersion parameters with the known tendencies to phase separation in the three (Li, Na, K) alkali silicates and support the correlations with observations on the nonideality-suppressing effects of  $\text{Al}_2\text{O}_3$  additions. This treatment leaves open the question of dielectric (or modulus) dispersion in ideally mixing or single-component conducting glasses. No information on the form of the loss spectrum and its dependence on composition was given.

Returning to the use of electrical modulus spectra and their comparison with corresponding responses to other perturbations, we note the special convenience of the finding (typified by Figures 3a and 4) that the spectra have a constant shape and that the  $f_{\text{max}}$  value is Arrhenius in temperature. It means that the shape of the isothermal relaxation spectra (on which theoretical models are tested) can be reproduced from a constant-frequency, variable-temperature experiment by

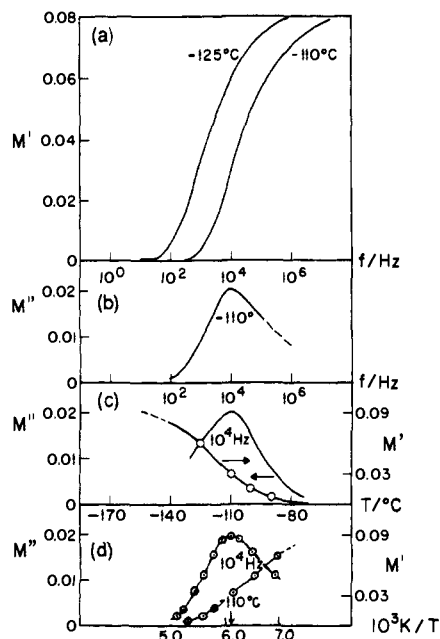


**Figure 5.** (a) Real parts of the electrical modulus for the superionic glass  $0.6\text{AgI}\cdot 0.4\text{Ag}_2\text{B}_4\text{O}_7$  measured at  $-110$  and  $-125$  °C. (b) Imaginary part of the electrical modulus for the same system measured at  $-110$  °C. Note maximum loss at  $10^4$  Hz for  $T = -110$  °C. (c) Real and imaginary parts of the electrical modulus for the same system at a constant frequency of  $10^4$  Hz measured as a function of temperature. (d) Real and imaginary parts of the electrical modulus for the same system plotted vs reciprocal temperature. Note identical shape of  $M''$  in parts b and d. The scale factor converting  $1/T$  units to  $\log f$  units is  $E_a/2.30R$ , where  $E_a$  is the activation energy for the relaxation process.

plotting  $M''$  vs  $1/T$ . This is because such a plot is effectively a plot of  $M''$  vs  $\log(\omega\tau)$  with  $\omega$  constant and  $\tau = \tau_0 \exp(E_a/RT)$ : the scaling coefficient between  $\log f$  and  $1/T$  scales is therefore  $E_a/R$ . Its utility is demonstrated directly by the alternative plots of data for the superionic glass  $3\text{AgI}\cdot 2\text{Ag}_2\text{B}_4\text{O}_7$ <sup>36</sup> shown in Figure 5. The equivalence of constant- $T$  and constant-frequency data representations shown by Figure 5 means that mechanical relaxation processes, which can only be studied in narrow frequency ranges in most laboratories, can be compared with electrical relaxation processes in the same system using  $1/T$  data representations<sup>16a</sup> and the differences then related to probable differences in *isothermal* relaxational functions.

Before testing the usefulness of this observation (see section IV), it is necessary to comment on the different types of mechanical relaxation measurements commonly made, since the modulus whose relaxation is being monitored varies from experiment to experiment. The *torsion pendulum* measurement follows the shear modulus  $G^*$  directly, the *Rheovibron* measures Young's modulus (the tensile modulus)  $E^*$ , and *ultrasonic* and *hypersonic* (by Brillouin scattering) *absorption and dispersion* studies follow either  $G^*$  or the longitudinal modulus  $M_1^*$ , depending on the cut of the exciting crystal (ultrasonic) or the particular phonon studied (Brillouin scattering).  $E^*$  and  $M_1^*$  are analyzable as different combinations of the fundamental moduli, bulk and shear,  $K^*$  and  $G^*$ , according to the relations

$$E^* = G^* \left[ \frac{3K^* - 4G^*}{K^* - G^*} \right] \quad (5)$$

$$M_1^* = K^* + \frac{4}{3}G^* \quad (6)$$

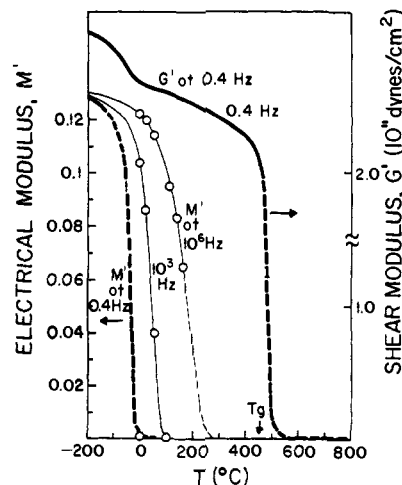


**Figure 6.** Variation of mechanical shear modulus (measured at 0.4 Hz) through fast and slow relaxation domains compared with that of the electrical modulus (measured at the same frequency). Note how the electrical modulus vanishes above the fast relaxation. (Data from refs 35 and 47 (solid lines) and from their extrapolations (dashed lines)).

It can be seen from eqs 5 and 6 that in the liquid state, where the shear modulus  $G^*$  vanishes,  $M_1^*$  will remain finite but  $E'$  will also vanish. The electrical modulus  $M_{el}'$  vanishes at a temperature *well below*  $T_g$  in all except insulating glasses. These relationships are illustrated for the case of  $\text{Na}_2\text{O}\cdot 3\text{SiO}_2$  in Figure 6 for electrical and mechanical measurements made at a common constant frequency of 0.4 Hz. Figure 6 also shows why it is acceptable, in comparing the results of mechanical with electrical relaxation data, to use the quantity  $\tan \delta$  ( $\tan \delta = E''/E'$  or  $G''/G'$ ) which is given directly by the experiment (rather than to make the extra measurements needed to obtain  $E'$ , in order to obtain  $E''$  separately). The reason is that  $G'$  and  $E'$  only change by 10% or less through the dispersion region, so the distortion of the spectrum introduced by use of  $\tan \delta$  instead of  $E''$  etc. is not serious.

#### IV. Dependence of Glassy Dynamics on Thermal History

In Figure 1 we illustrated the effect that thermal history can have on the state of a molecular glass as indicated by its density. It is easy to imagine that such a density difference in an ionic glass could have a profound effect on the ability of small loosely bound particles to migrate through the structure: hence, the *average relaxation time* for a glassy-state relaxation should depend on the thermal history. We have already seen in Figure 4 that in a glass, i.e., an amorphous phase of fixed structure, the relaxation *function* for electrical stresses is independent of temperature. But is this function dependent on the *particular* structure frozen in, and hence on the thermal history? Such a question is surely one of the first that should be answered concerning glassy dynamics.

It is interesting, in this respect, to examine how the relaxation function for a fast process, the electrical relaxation, varies with changing structure in the metastable *liquid* (ergodic) state as opposed to the non-ergodic glassy state. Since a glass is frequently characterized by its fictive temperature (i.e., by the temperature at which some property, e.g., the enthalpy, is

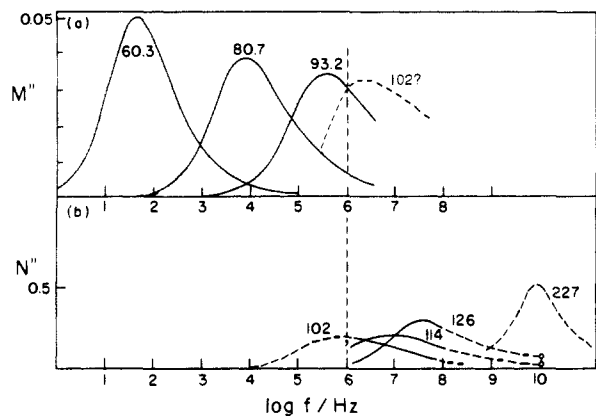


**Figure 7.** Comparison of loss spectra and their temperature dependences for electrical and mechanical relaxations in liquid  $3\text{KNO}_3 \cdot 2\text{Ca}(\text{NO}_3)_2$ . Note that (i) at the same temperature, 102 °C, electrical relaxation is shorter (peak frequency higher) than the mechanical relaxation and (ii) the electrical relaxation spectrum narrows with decreasing temperature while the mechanical relaxation broadens.

the value for the ergodic state), it seems likely that the variations to be observed in the liquid will be those applying to the different frozen-in structures. Unfortunately, there are relatively few studies of electrical and/or mechanical relaxation in the ionic liquid state to serve as guidance. However, those that exist<sup>26,38-42</sup> are provocative and prove to have predictive value.

The usual behavior observed for the primary mechanical (*structural*) relaxation in the liquid state is one of increasingly non-Arrhenius average relaxation time, and increasingly nonexponential relaxation (i.e., decreasing  $\beta$  in eq 1), as temperature decreases. Typical is the behavior of the normalized longitudinal modulus for  $3\text{KNO}_3 \cdot 2\text{Ca}(\text{NO}_3)_2$  depicted in Figure 7b based on ultrasonic,<sup>39</sup> Brillouin scattering,<sup>40</sup> and recent digital correlation spectroscopy data.<sup>41</sup> Since the electrical relaxation time shows a comparable temperature dependence, similar spectral width behavior might have been expected for the electrical modulus. However, at least in the vicinity of  $T_g$  the opposite is found, according to the study of Howell et al.,<sup>24a</sup> whose results are shown in Figure 7a. The generality of this result, which has been correlated with aspects of the conductivity temperature dependence,<sup>16a</sup> is suggested by a similar narrowing seen with decreasing temperature for three mineral acid glass-forming systems by Hodge and Angell.<sup>42</sup> In each case the spectral width became fixed for  $T$  less than  $T_g$ , but the results clearly suggest that annealing the glass to a lower fictive temperature (enthalpy state) should result in a spectral narrowing.

A short extrapolation of the variation of  $\beta$  with temperature in the liquid state of  $3\text{KNO}_3 \cdot 2\text{Ca}(\text{NO}_3)_2$  (see Figure 8) suggests a value of unity (exponential relaxation) would be achieved at a temperature of 28 °C, 301 K, at which  $T_g/T = 1.12$ . In this case,  $T_{\beta \rightarrow 1}$  corresponds to the Kauzmann temperature (if we may judge by  $T_g/T_K$  for the compound-forming liquid  $\text{BiCl}_3 \cdot 2\text{KCl}$  of the same fragility as  $2\text{Ca}(\text{NO}_3)_2 \cdot 3\text{KNO}_3$ <sup>43</sup>). This is particularly intriguing since several recent studies on the nonexponentiality of the *primary* relaxation in fragile liquids have suggested that  $\beta \rightarrow 0$  at the Kauzmann temperature.<sup>44</sup> The conductivity behavior reflects the decreasing concentration of mobile cations in the increasingly dense structure, and hence the decrease in

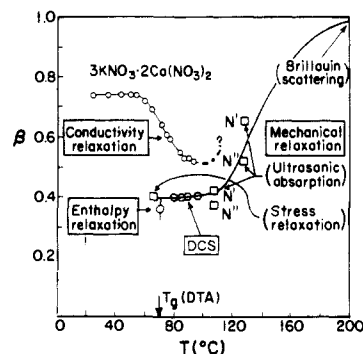


**Figure 8.** Contrasting temperature dependences of the KWW  $\beta$  parameter for (fast) electrical relaxation and (slow) mechanical relaxation processes for the system  $3\text{KNO}_3 \cdot 2\text{Ca}(\text{NO}_3)_2$  from various data sources.<sup>8,24,39,41,88b</sup>

the charge-charge interactions which may be the source of the nonexponentiality of the conductivity relaxation.<sup>45</sup>

The dependence of conductivity relaxation on fictive temperature in the ionic glasses may be compared with the effect of aging on secondary relaxation in molecular glasses.<sup>13</sup> In the latter, the reduction in the number of mobile units participating in the relaxation causes a decrease in  $\Delta\epsilon$  rather than in the relaxation time or nonexponentiality.

Although no annealing studies (or for that matter quenching studies) have been carried out on  $3\text{KNO}_3 \cdot 2\text{Ca}(\text{NO}_3)_2$  to confirm or deny the suggested state dependence of the spectral width of the fast process in the *glass*, some data are available for a sodium silicate glass studied by Boesch and Moynihan.<sup>46</sup> These authors showed that on annealing, the width of the electrical loss peak  $M''$  did indeed decrease in the manner expected from the above observations. Although the change in  $\beta$  for a 6% change in reduced fictive temperature,  $\Delta T_f/T_b$ , is much smaller in this system than in  $\text{Ca}/\text{K}/\text{NO}_3$ , so is the change in  $\sigma$  itself. However, if we normalize by the change in  $\sigma$  produced by the change in fictive temperature, the effects are comparable. This is consistent with a charge-charge interaction origin for the nonexponentiality of the conductivity relaxation.

Effects in the same direction have been seen recently by Mangion and Johari<sup>37</sup> for the case of  $\text{AgPO}_3$  glass. In this case, however, some structure developed in the  $M''$  spectra during the annealing. This subject merits more attention.

The unusual behavior of the conductivity relaxation with fictive temperature naturally raises the question of whether or not the *mechanical* loss, which must be associated with the mobile ion relaxation, shows spectral width variations similar to those of the electrical relaxation (fast process) rather than to those of the structural relaxation (slow process). We compare electrical with structural relaxations in the same glass in the next section.

## V. Comparison of Electrical and Mechanical Relaxation Spectra

In section III, it was pointed out that the combination of temperature-independent spectral width and Arrhenius temperature dependence of the peak frequencies found in electrical relaxation of glasses meant that



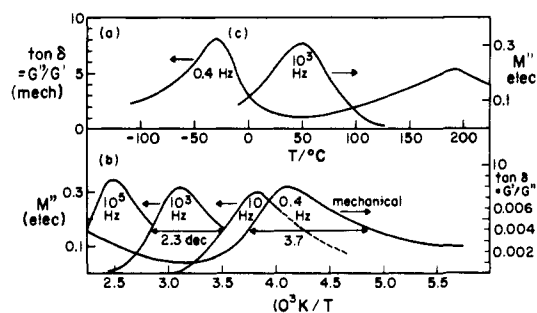


**Figure 9.** (a) Mechanical loss for  $\text{Na}_2\text{O}\cdot 3\text{SiO}_2$  glass at fixed frequency and varying temperature. Low-temperature component is due to  $\text{Na}^+$  ion motion. (b) Comparison of "spectrum" for mechanical relaxation of  $\text{Na}_2\text{O}\cdot 3\text{SiO}_2$  using  $1/T$  representation with equivalent electrical relaxation spectra showing small differences in peak loss position and large difference in half-width.

the shape of the isothermal relaxation spectrum could be obtained from constant-frequency measurements by plotting the moduli vs  $1/T$ . This implied that comparisons with the frequency-limited mechanical relaxation functions could be made by using the  $1/T$  representations of the data. This is done for the case of  $\text{Na}_2\text{O}\cdot 3\text{SiO}_2$  glass in Figure 9, where mechanical (shear modulus) data taken at 0.4 Hz over a range of temperatures<sup>47</sup> (Figure 9a) are compared in the  $1/T$  representation with isothermal electrical relaxation spectra of Figure 4. It is seen immediately that the mechanical relaxation spectrum is considerably broader than the electrical relaxation spectrum, which is itself constant in half-width. We will see that this increased spectral width for mechanical relaxation is a recurring feature of processes associated with mobile ion motion in ionic glasses. Before giving more detailed consideration to the description of these shapes, we need to present evidence for the suggestion that the mechanical, like the electrical, relaxation has a temperature-independent spectrum.

Allusion was made above to exceptions to the restricted frequency range of mechanical measurements. The development of a sensitive mechanical spectrometer at the Institut National des Sciences Appliquées in Lyon<sup>48</sup> has made possible the measurement of isothermal mechanical relaxation spectra over 3–4 orders of magnitude in frequency. Such measurements permit a check of the validity of attributing differences in  $1/T$  "spectra" (as in Figure 5) to differences in the isothermal relaxation function, by showing that the shapes of isothermal mechanical relaxation spectra are also independent of temperature. This is done in Figure 10 for the case of a five-component heavy-metal fluoride glass (based on  $\text{ZrF}_4\text{-BaF}_2$ , the "ZBLAN" modification), in which the mobile particles are the fluoride ions (or at least a fraction of them), using the data of Mai et al.<sup>49</sup> The figure presents both electrical and mechanical data for several different temperatures. The individual isotherms have been superimposed by shifting along the frequency axis so that the peaks coincide. The finding that a single master plot can be obtained argues that the spectral shape is temperature independent for mechanical as well as for electrical relaxation processes in this system. Since this was approximately the case in an earlier wide frequency range study of mechanical relaxation in a mixed-alkali silicate glass,<sup>50a</sup> it seems likely that this finding will be general, as for electrical relaxation. In this case the analysis of constant-fre-

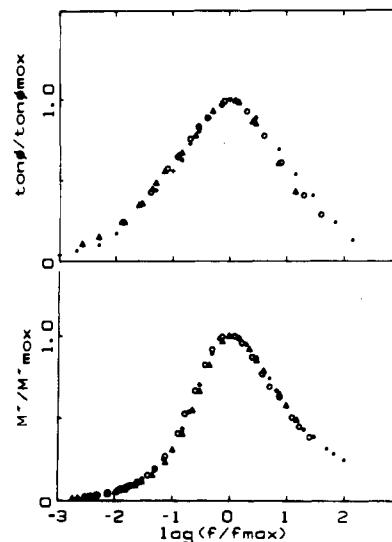


**Figure 10.** Master plots for electrical and mechanical relaxation in an anion-conducting ( $\text{F}^-$ ) heavy-metal fluoride glass. Reprinted from ref 28; copyright 1985 Taylor & Francis Ltd.

quency data using the  $1/T$  representation will be of general utility.

The heavy-metal fluoride glass is an interesting case because the half-width of the mechanical relaxation is not much greater than that of the electrical relaxation (although the shape is clearly different). This is possibly to be correlated with the fact that the fluoride glass is a rather poor ionic conductor: its decoupling index is only of the order of  $10^8$  at  $T_g$  compared with  $10^{11}$  for  $\text{Na}_2\text{O}\cdot 3\text{SiO}_2$ . As for the case of  $\text{Na}_2\text{O}\cdot 3\text{SiO}_2$ , the shape of the electrical relaxation spectrum is very well fitted by the Williams–Watts function. The KWW  $\beta$  value is 0.61, somewhat larger than the value of 0.55 fitting the  $\text{Na}_2\text{O}\cdot 3\text{SiO}_2$  data of Figure 9 and smaller than the value 0.74 fitting the glass state data for  $3\text{KNO}_3\cdot 2\text{Ca}(\text{NO}_3)_2$  (see Figure 8). The order of  $\beta$  values is the inverse of the order of decoupling indexes. This is a very significant correlation, which we will discuss more quantitatively below.

It is clear from Figure 10 that the mechanical relaxation in this fluoride glass, despite the similar half-width to the electrical case, is not well described by the KWW function. In fact, its asymmetry with respect to the ideal Lorentzian form is the opposite of that for the conductivity relaxation. A similar distortion was observed by Liu and Angell for the case of  $\text{AgI-AgPO}_3$  glasses,<sup>50b</sup> though in this case the mechanical spectrum was much broader than the electrical. On the other hand, Ngai, in an exhaustive review of the older oxide glass literature,<sup>16b</sup> found that the mechanical spectrum could always be satisfactorily fitted with a KWW function and that in at least one case<sup>51</sup> the  $\beta$  value decreased markedly on annealing. This is the opposite of the behavior observed for the conductivity relaxation and is more akin to the behavior of the slow relaxation in molecular glasses.<sup>52</sup> The mechanical spectrum for these poorly conducting glasses was always much broader than that observed for the conductivity relaxation of the same glass (and is, in fact, always broader than the broadest electrical relaxation observed in any ionic glass at all).

As a final example we present data for a superionic conducting system,  $3\text{AgI}\cdot 2\text{Ag}_4\text{B}_2\text{O}_7$ ,<sup>53</sup> which has a decoupling index of  $\sim 10^{14}$ . Data for mechanical and

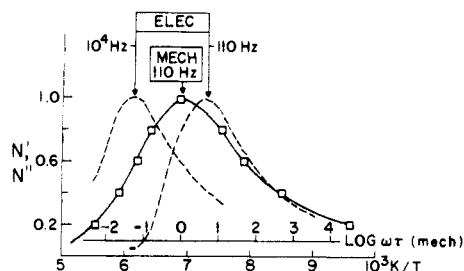


**Figure 11.** Comparison of electrical and mechanical relaxation spectra using  $1/T$  representations of constant-frequency data. The spectrum is well described by a KWW function (eq 3) with  $\beta = 0.29$ . The electrical relaxations, which have almost the same peak temperature for the same frequency, are also of KWS form but are much narrower ( $\beta = 0.48$ ).

electrical relaxation<sup>38</sup> are shown in the  $1/T$  representation in Figure 11. It is clear from Figure 11 that the mechanical relaxation is again much broader than the electrical relaxation, though they can each be well described by KWW functions in contrast with the case of Figure 10. Since other examples are known in which the superionic glass mechanical relaxation is both broader and more symmetrical (non-KWW) than the electrical relaxation, it seems that at this time there are no general rules for the relationship except that the most probable times are similar and that the mechanical process is nearly always broader. We defer possible explanations until a later section.

For future studies, more cases are needed in which the (fast) mechanical relaxation function is well separated from the primary (slow) structural relaxation function so that the difficulty of deciding the appropriate background subtraction can be reduced. It is desirable also that the behavior with changing fictive temperature, preferably within the liquid state as pioneered by Torell,<sup>54</sup> can be determined and compared with the behavior seen in Figure 6. Favorable cases would seem to be the superionic systems  $3\text{AgI}\cdot 2(\text{Ag}_2\text{O}\cdot 2\text{B}_2\text{O}_3)$ <sup>53</sup> and "NaSi glass" ( $\text{Na}_{3.75}\text{Zr}_{1.1}\text{Si}_{2.75}\text{P}_{0.25}\text{O}_{10.2}$ )<sup>55</sup> which have decoupling indexes at  $T_g$  of  $10^{13.5}$  and  $10^{14.1}$ , respectively.<sup>24</sup> Some sulfide glasses studied by Ribes and colleagues<sup>56-58</sup> and by Kennedy and co-workers<sup>59,60</sup> which have exceptionally high room temperature conductivity and relatively high  $T_g$ s may also be suitable. In addition, we must note the recently reported case of exceptional conductivity in the system  $\text{CuI}\text{-Cu}_2\text{O}\text{-MoO}_3$ . Minami and Machida<sup>61</sup> report  $\sigma_{298}$  values 10–20 times greater than their AgI equivalent, though a restricted glass-forming range limits the final maximum conductivity observable.

To complete this section, we must refer to the dynamic peculiarities of the *mixed* mobile ion glasses, i.e., glasses in which special features develop because more than one ionic species is free to move. The most celebrated case is the so-called "mixed-alkali" effect in which the mixing of two alkali oxide glasses (silicate, borate, phosphate, etc.) of comparable conductivity results in a glass of conductivity orders of magnitude lower than either.<sup>62</sup> The width of the electrical relaxation in the mixed glass does not seem much affected, though its peak frequency decreases greatly.<sup>63</sup> The mechanical spectrum, on the other hand, is greatly affected. From torsion pendulum studies,<sup>64</sup> a new intense loss peak ( $\tan \delta$ ) appears at lower frequency on small additions of the second alkali and, partly because

of its strength, completely overwhelms (if not annihilates) the single-alkali peak.<sup>64</sup> This peak falls at a frequency some 1.5 orders of magnitude below the frequency of the conductivity loss peak, whereas for single-alkali glasses the two loss peaks have essentially the same peak frequency. The mixed-alkali effect has been much discussed in the glass science literature, and the reader is referred to the paper by Ingram and Moynihan<sup>65</sup> for a current, if not yet generally accepted, explanation.

Several other "mixed-ion" effects have been noted, but their spectroscopic characterization is not yet very advanced. A mixed-anion effect that enhances rather than depresses conductivity has been observed in cation-conducting glasses such as  $\text{GeS}_2\text{-LiBr-LiI}$ <sup>66</sup> and  $\text{CuI-CuBr-Cu}_2\text{MoO}_4$ .<sup>61</sup> In anion conductors, on the other hand, mixing of anions produces depressed conductivities as in the mixed-alkali case.<sup>61,66</sup> Finally, in a mixed cation-anion conducting system,  $\text{LiF}_2\text{-PbF}_2\text{-Al(PO}_3)_3$ , the conductivity is depressed on mixing at a constant 20%  $\text{Al(PO}_3)_3$ . In this latter case, some spectroscopic data are available.<sup>67</sup> By contrast with the mixed-alkali glass, the conductivity relaxation spectrum broadens anomalously at mid range where the change-over from cation to anion dominance is expected, while the mechanical loss *decreases* from the pure alkali glass value on mixing. This is a research area where additional studies are needed and from which important and diagnostic correlations may emerge.

## VI. Comparison of Electrical and Nuclear Magnetic Relaxation Data

In view of the differences observed in mobile ion glass responses to electrical and mechanical perturbations, it is of interest to observe what information may be obtainable on the relaxation function from nuclear magnetic relaxation measurements. In these studies the nuclear spin system, which is only very weakly coupled to the nuclear coordinate system, i.e., to the glass or liquid structure, is perturbed by a magnetic field, and the reestablishment of the spin equilibrium is monitored by a radiofrequency detection technique tied to the precession of the active nuclei in the magnetic field. The typical measurement, analogous to the typical mechanical spectrometry measurement, uses a fixed probe frequency determined by the intensity of the magnetic field in which the sample is placed and scans in temperature. The response of the system, for the case on which we focus attention, is measured as the spin-lattice relaxation time  $T_1$ . This has a minimum value when the atomic system to which the spectrometer is tuned has a decay time for structural fluctuations  $\tau_c$  approximately equal to the inverse spectrometer frequency, i.e.,  $\omega\tau_c \approx 1$ .

The method is applicable for any system containing nuclear species with a magnetic moment but is particularly suitable for systems with favorable (spin  $1/2$ ) nuclei such as  $^{23}\text{Na}$ ,  $^7\text{Li}$ ,  $^{19}\text{F}$ , and  $^1\text{H}$ , which happen to be species of special interest in ionic glass dynamics phenomenology.

Until recently, most analyses of the  $T_1$  temperature dependence in glasses<sup>69-71</sup> had been used on the Bloembergen, Purcell, and Pound (BPP) theory,<sup>68</sup> which assumes an exponential decay for the structural fluctuations involved in helping the spin system recover its

equilibrium state. It was recognized that the shape of the  $\log T_1$  vs  $1/T$  plot deviated from that expected from BPP theory. Although it was not obviously connected to the weakness of the theory, it was also found<sup>69</sup> that the activation energy for the plot of  $\log T_1$  vs  $1/T$  was not the same as for the dc conductivity;<sup>70</sup> it had been expected that the nuclear motions involved in relaxing the spin system would be the same as those involved in determining the dc conductivity. Furthermore, the prefactor found for the fluctuation correlation time,  $\tau_c$ , Arrhenius law was unphysically low.

The origin of all these discrepancies has now been shown to lie in the inappropriateness of the BPP exponential relaxation assumption. Göbel et al.<sup>71</sup> showed that for various alkali silicate and borate glasses the asymmetric shape of the  $\log 1/T_1$  vs  $1/T$  plot could be well accounted for if the fluctuation frequency spectrum were assumed to follow the Cole–Davidson distribution. A more recent example, using data that extend further above the  $T$  minimum, is given by Pradel and Ribes.<sup>72</sup> Ngai<sup>73</sup> demonstrated that an equally good fit followed from use of the KWW function, so that NMR data showed yet another example of the near-universal occurrence of KWW (or, as aptly named,<sup>74</sup> “fractal time”) character of fluctuation decay in disordered systems. A new example of the KWW fit, using  $T_1$  data for  $\text{Li}_2\text{S}-\text{SiS}_2$  glass, is given by Martin<sup>75</sup> in an excellent account of current developments in the subject. The relation between constant-frequency ac conductance and constant-frequency NMR studies, the study of which clarifies the origin of the depressed activation energy and unphysical prefactor found in the NMR studies, is considered in articles by Ngai,<sup>16b,73b</sup> Angell,<sup>25b,76</sup> Angell and Martin,<sup>77</sup> and Martin.<sup>75</sup>

The question immediately arises, is the departure from exponential relaxation seen in NMR closer to that for conductivity or that for mechanical relaxation? In both the lithium borate glass examined by Ngai<sup>73</sup> and the superionic lithium thiosilicate glass fitted by Martin,<sup>75</sup> it seems that the  $\beta$  value coincides with that for ac conductivity. The conductivity values, which seem to be much more reproducible and systematic in character than their mechanical equivalent, would thus seem to be the values that we should first seek to correlate with other structural and relaxational features of the system. This will be the subject of the next section. Before passing to this section, however, we should give brief attention to the origin and meaning of the low value of activation energy for NMR relaxation obtained from the  $\log T_1$  (or  $\log T_1^{-1}$  as commonly plotted) vs  $1/T$  plot below the temperature of the  $T_1$  minimum, since this is currently subject to different interpretations.

Angell<sup>25b,76</sup> and Angell and Martin<sup>77</sup> have argued, by analogy to the much-studied case of frequency-dependent (ac) electrical conductivity, that the low activation energy relative to that for dc conductivity is a straightforward consequence of the fact that measurements have been made in a temperature range where  $\omega\tau > 1$  in the presence of nonexponential relaxation. In ac conductance measurements, the activation energy agrees with the value obtained from dc measurements only so long as the period of the ac field is long compared with the ion jump time (or, more correctly, the conductivity relaxation time). Since low-frequency measurements are easily accessible with admittance

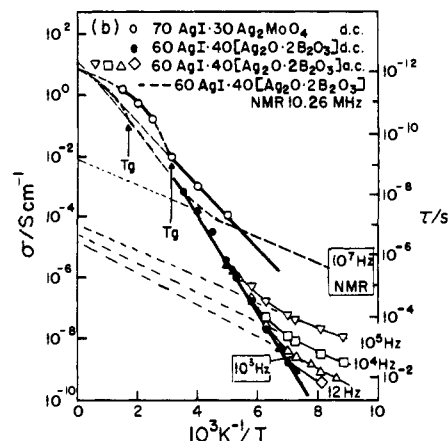


**Figure 12.** Arrhenius plot of ac conductivity (and relaxation times determined from it by a Maxwell relation valid only for conductivity measured where  $\omega\tau \ll 1$ ) compared with NMR correlation times determined from data where  $\omega\tau < 1$ . Note that in both cases, NMR and low-temperature conductivity, the activation energy is well below the dc conductivity value, and the prefactor not only is unphysical but is frequency dependent. Both results are due to invalid data treatments that assume exponential relaxation.

bridges, it is easy to satisfy this requirement (hence most studies of dc conductivity are made by using ac techniques). When the jump time becomes longer than the inverse bridge frequency, a departure from the dc conductivity Arrhenius plot occurs, as shown for the case of the  $60\text{AgI}-40(\text{Ag}_2\text{B}_4\text{O}_7)$  superionic conductor<sup>38</sup> in Figure 12. The temperature of the break depends, of course, on the bridge frequency held constant. If we plot the data as *apparent* relaxation times using the relationship applicable to the dc conductivity (see eq 1)

$$\tau_\sigma = e_0/M_\infty\sigma \quad (7)$$

we obtain plots (see Figure 12) that extrapolate to  $1/T = 0$  at  $\tau_0$  values (the Arrhenius law prefactor) that are even lower (hence more unphysical) than those found in the NMR studies. However in the ac conductivity case the reason is well understood, following Macedo et al.,<sup>23</sup> as a consequence of the fact that the conductivity (or coupled conductivity/dielectric<sup>29</sup>) relaxation is nonexponential. In this interpretation the (lower) ac “activation energy” has no meaning except as an indicator of the extent of departure from Debye relaxation. As a way of demonstrating that the low activation energies for the BPP correlation time,  $\tau_c$ , and the low prefactors obtained from the NMR studies have the same explanation, we include in Figure 12, as a dashed line marked “ $10^7$  Hz NMR”, a plot for NMR  $\tau_c$  data interpolated from results presented for  $\text{AgI}-\text{Ag}_2\text{B}_4\text{O}_7$  glasses of compositions 50 and 70% AgI by Martin et al.<sup>78</sup> The activation energy is seen to be similar to that for the ac conductivity. The main difference is that, due to the high spectrometer frequency, the onset of frequency-dependent behavior occurs at a higher temperature, so the prefactor found is higher than for the ac conductivity.

In this interpretation, the plot of  $\log 1/T_1$  vs  $1/T$  (e.g., Figure 4, in ref 72, for the case of  $\text{Li}_2\text{S}-\text{SiS}_2$ ) should be regarded as the NMR equivalent of the modulus,  $M''$ , plots of Figures 5d and 11. (Accordingly, a plot of  $\log M''$  vs  $1/T$  for  $T$  above the  $T_1$  minimum yields an activation energy close to, but still somewhat smaller

than, the dc conductivity value. Agreement will only be quantitative when  $\beta = 1$ .) The equivalent of the persistent high-frequency loss causing deviations from the form predicted by KWW for the modulus at high frequencies (see section VIII) is the residual  $T_1^{-1}$  commonly seen in the low-temperature NMR data.<sup>71,79</sup>

An alternative interpretation of the low-temperature NMR data has been given by Ngai and co-workers.<sup>80</sup> They argue that the activation energy from  $T_1$  data obtained well below the  $T_1$  minimum is a microscopic activation energy of fundamental importance to understanding glassy-state dynamics. It represents, in their view, the activation energy for a "primitive" process initiated by perturbing stress, i.e., the relaxation at very short times before a coupling to the complex environment acts to slow down the relaxation rate and thus to lead, in the coupling model,<sup>16,81</sup> to the KWW behavior of the complete relaxation. In support of this argument they show a good agreement between the  $T_1$  activation energy and the quantity  $\beta E_\sigma$ , where  $\beta$  is the KWW exponent from electrical relaxation studies and  $E_\sigma$  is the dc conductivity activation energy. This product is the value for the "primitive" process activation energy according to the coupling model, i.e., the value before "the slowing down of one primitive relaxing rate  $\omega_0$  to  $\omega_0(\omega_c t)^{1-\beta}$  by cooperative interactions with other ions", which seems to be ubiquitous in glasses, takes over. (This work also emphasizes the sublinear frequency dependence observed at  $\omega\tau \gg 1$  and gives an interpretation that is relevant to our discussion of connection between relaxation and vibrational modes given in section VIII.)

Clearly, this research area is in a state of active development and, with variable-frequency NMR being actively pursued,<sup>75</sup> much additional insight into the dynamics of ionic processes in glasses will soon be forthcoming.

The silver iodoborate case used in the above discussion has also been the subject of some very wide frequency range mechanical studies that make it of special value for analyses aimed at providing a unifying picture of the energy-dissipating processes in glassy ionic solids. We consider these in a final section after a brief but especially important section in which spectroscopic observations are tied into the broader phenomenology of slowing down in glass-forming liquids.

### VII. Correlation of Relaxation Spectra with Decoupling Index and Structure

Having reviewed the main spectroscopic characteristics of dynamic processes in ionic glasses, we now turn to the important matter of correlating the findings with the broader phenomenology of viscous liquids and the vitrification process.

We noted at the beginning of this review that the glassy-state processes we have been characterizing are actually spawned in the high-temperature *liquid* state. It has been known for a very long time that, in molten salts, the electrical conductivity has a characteristically different temperature dependence from the shear viscosity. Both processes,  $P_i$ , have been found<sup>82,83</sup> to obey the famous Vogel-Tammann-Fulcher equation

$$P_i = P_{0,i} \exp[\pm B_i/(T - T_0)] \quad (8)$$

where, subject to some provisos, the constant  $T_0$  is

identified with the Kauzmann vanishing excess entropy temperature,  $T_K$ ,<sup>83-85</sup> which stands as the low-temperature limit on the liquid state. According to the experiments, both processes respect the same limit,  $T_0$ , initially, but the conductivity has a smaller  $B$  parameter. Representing the processes by their average relaxation times,<sup>22</sup>  $\tau_\sigma$  and  $\tau_s$ , we see that the processes must separate increasingly in time as temperature decreases (as in Figure 2a,b), the rates of separation depending on the difference in their  $B$  parameters. Kawamura and Shimoji<sup>86</sup> have therefore suggested that the ratio  $B_s/B_\sigma$  may serve as a temperature-independent index of the decoupling of conductivity from structural (viscosity) modes in a given system. This has an obvious advantage over the "decoupling index",  $R_\tau = \tau_s/\tau_\sigma$ , used by Angell,<sup>25</sup> which, in most cases of interest, has a different value at each temperature. However, this advantage is partly offset by the finding<sup>87</sup> that eq 8 usually breaks down before the glassy state is reached, such that the two processes return to an Arrhenius temperature dependence while still in the liquid state. Furthermore, the return to Arrhenius behavior occurs at a higher temperature for conductivity than for viscosity and is system dependent. In view of these complications we will continue to use the decoupling index determined at the glass transition temperature in discussing the origin of the different  $\beta$  values observed for conductivity relaxation in earlier sections. However, in future work efforts should be made to develop the Kawamura-Shimoji suggestion since the  $B_i$  ratio can be given a theoretical interpretation. If a free volume approach<sup>86</sup> is adopted,  $B_s/B_\sigma$  is a measure of the difference in free volume requirements for conductive vs viscous motion or, if we invoke our current preference<sup>88</sup> for an Adam-Gibbs<sup>85</sup> entropy-based interpretation of the transport phenomena, it is a measure of the difference in energy barriers for rearrangement of the minimum-size rearrangeable group involved in relaxing an electrical stress as opposed to a mechanical stress.

In light of the above discussion it seems reasonable to expect the kinetic processes in the glassy state to reflect in some measure the extent of decoupling from the viscous modes achieved in the liquid before vitrification. The differences among different glasses in this respect may be presented, as in refs 25 and 86, by a tabulation of decoupling indices at  $T_g$ . These may be easily estimated by combining eq 1, in which we insert a typical value of  $M_\infty = 0.08$

$$\tau_\sigma = e_0/M_\infty\sigma_{dc} \approx 9 \times 10^{-13}/\sigma_{dc} \text{ s} \quad (9)$$

with the observation that, in general

$$\tau_s \text{ (at } T_g) \approx 2 \times 10^2 \text{ s} \quad (10)$$

so that

$$R_\tau \text{ at } T_g = \tau_s(T_g)/\tau_\sigma(T_g) \approx 2 \times 10^{14}\sigma_{T_g} \quad (11)$$

However, a better feeling is obtained for the extreme differences that exist between different systems by a graphical presentation of the conductivities over a wide temperature range using a reduced Arrhenius plot such that all glasses have the same structural relaxation time at the scaling temperature. The natural choice for scaling temperature is  $T_g$ . The plot is presented in Figure 13, which includes a dashed line to represent a system in which the conductivity and viscosity modes

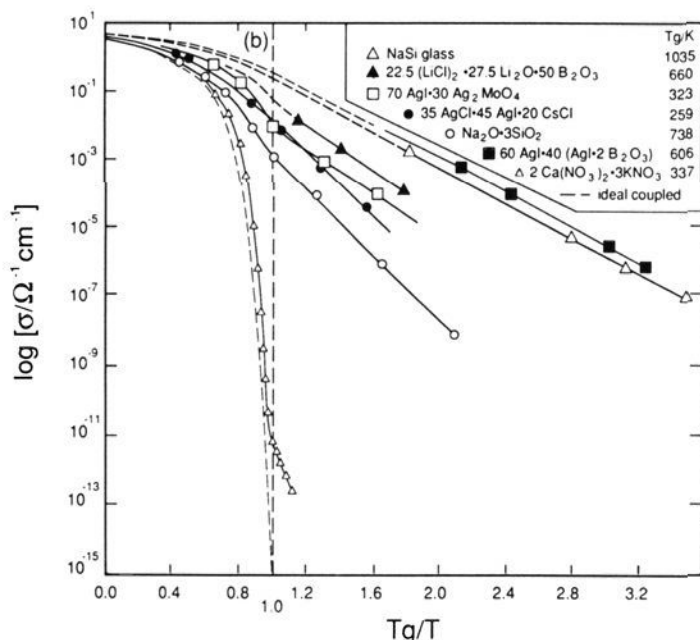


**Figure 13.**  $T_g$ -scaled Arrhenius plot of conductance of systems with widely differing degrees of decoupling of conductivity from structural modes. Dashed line shows behavior for fully coupled system.

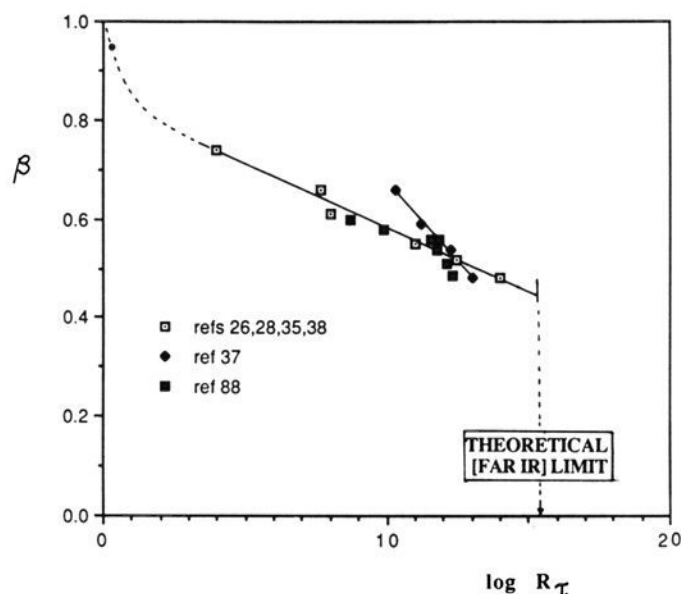


**Figure 14.** Correlation of nonexponentiality parameter  $\beta$  of Kohlrausch function with decoupling index  $R_\tau$  for a variety of ionic glasses.

remain fully coupled over the entire temperature range.

Figure 13 is very similar to the theoretical plot of Kawamura and Shimoji<sup>86</sup> for a system of fixed  $B_s$  (eq 8) being vitrified at a fixed rate, with variations in the value of  $B_\sigma$ . To this writer, the figure is quite evocative. It would seem surprising indeed if the extremely different time scales for electrical relaxation relative to a constant time scale for relaxation of mechanical stress were not reflected in some way in the spectroscopic characteristics of the conductivity relaxation in the glass. Thus we check in Figure 14 what seems the obvious correlation to investigate (but one not presented previously), viz., correlation of the nonexponentiality parameter  $\beta$  (in the glassy state) with the decoupling index  $R_\tau$  at  $T_g$  (since  $T_g$  is where the bulk structure becomes arrested).

Despite the presence of some system-specific irregularities, Figure 14 shows a rather definite relationship: the more fully decoupled the conductivity at  $T_g$ , the more nonexponential the relaxation. There would seem to be a well-defined limit for  $\beta$  in ionic conducting systems since the theoretical limit for  $\sigma_T$  is given by the far-infrared conductivity,  $\sim 10 \text{ S cm}^{-1}$ .<sup>24,90</sup> Thus the limiting value of  $R_\tau(T_g)$  should be  $\sim 10^{15.4}$ , and hence the limit on  $\beta$  should be 0.44. Broader spectra may be obtainable by overlapping independent processes, as

seems to happen near the mobile ion crossover in mixed mobile ion systems,<sup>67</sup> or in the presence of incipient phase separation, but such cases would always have a special explanation. The rapid decrease in  $\beta$  at the left-hand side of the diagram (based on data in dilute alkali silicates and germanates) has been interpreted by Martin<sup>75</sup> in terms of the rapid change in cation-cation separation.

A correlation of  $\beta$  with another system parameter that is as impressive as Figure 14 (though, to the present author, a little less provocative) is that described by Ngai and Martin.<sup>80b</sup> These authors modify an earlier correlation<sup>89</sup> of  $\beta$  with dc conductivity activation energy  $E_a^*$  by converting  $E_a^*$  to a "primitive" activation energy  $\beta E_a^*$  and plotting this against  $\beta$  (actually against  $n = 1 - \beta$ ) and are able to superpose data from many different systems. While the presence of  $\beta$  on both axes aids the correlation somewhat, it is theoretically justified.

To interpret these observations further, one should ask what Figure 14 implies about the structure within which the mobile ion displacements are occurring and consider this in relation to current models for nonexponential relaxation.

It is tempting to answer this question in terms of microheterogeneity models.<sup>90-92</sup> In such models it is supposed that the viscosity and structural relaxation are controlled by the approach to percolation of growing clusters of dense-packed material, while the intercluster matter, in which conductivity occurs, remains relatively loose and liquid-like. This picture is essentially that invoked in the "cluster bypass" model for high ionic conductivity advanced recently by Ingram.<sup>93</sup> It is orthogonal to the widely espoused " $\alpha$ -AgI cluster overlap" model<sup>94</sup> which explains the tendency of most AgI-containing glasses to approach the properties of  $\alpha$ -AgI crystals as AgI content increases in terms of overlap of growing clusters of mobile material (but which seems inconsistent with the similar behavior of  $\text{Ag}_2\text{S}-\text{AgPO}_3$  glasses<sup>95</sup>). This general picture emphasizing loose intercluster material is also consistent with recent evidence that, in many, though certainly not all, "fragile" liquids, the time scales for shear relaxation and structural or enthalpy relaxation begin to separate as  $T_g$  is closely approached.

The connection to Figure 14 by models for nonexponential relaxation could then be made in at least two ways. Both depend on the idea that in the highly decoupled, i.e., large  $R_\tau$  systems, the matrix material of the cluster bypass model must be particularly liquid-like and/or perhaps involve a particularly large proportion of the mobile, low-charged, ions in the structure.

(1) In the "coupling" model of Ngai and colleagues,<sup>16,97</sup> the departure from exponentiality (quantified by  $n = 1 - \beta$  in their model) is a function of the level of disorder in the environment of the "primitive species", which should be greater in a highly decoupled system matrix. We note the success of this model in explaining the isotope effect in alkali borate glasses<sup>98,99</sup> and suggest such experiments be repeated for the systems representing the accessible extremes of the decoupling phenomenon.

(2) In the Tomazawa model,<sup>45a</sup> which is specific to the behavior of ionic systems, the explanation of the greater departure from exponentiality in highly decoupled

glasses would follow directly from the larger concentration of mobile species in matrix material. This is also the view of Martin.<sup>75b</sup> The source of their nonexponential relaxation is the well-known Debye-Falkenhagen effect, which, however, can only account quantitatively for the first 5% increase in spectral width (hence the initial drop in  $\beta$ , Figure 14) according to Lesikar and Moynihan.<sup>96</sup> A more recent analysis by McGahay and Tomazawa<sup>45c</sup> goes some way toward removing this limitation.

It should be very interesting, in this respect, to study the spectroscopic characteristics of conductivity in the ultrafast quenched glasses of Tatsumisago et al.<sup>100</sup> in which the fraction of mobile material in the structure should be maximized.<sup>96</sup> Also lacking in the present data base are oxide glasses designed to be insulating glasses—e.g., alkali-free lead or barium silicates.

### VIII. Connections between Relaxational and Vibrational Responses

In the foregoing sections we have reviewed the detailed kinetics of various processes that occur within the "frozen" glass structure and have attempted to connect their characteristics to the process by which they form. While they are spawned in the high-temperature liquid where all relaxation times are short, they have their own short- and long-time characteristics. Most of the studies reviewed to date have been concerned with the medium to long time regime. It is of considerable interest to investigate the behavior of the glassy-state processes, both mechanical and electrical, as the frequency range of the measurement approaches the microscopic short-time (vibrational) limit. Thanks to the existence of some glasses in which the conductivity mode decoupling is exceptional, it is possible to extend the glassy-state studies to within three decades of the typical vibrational frequency. Because of the value we place on the conceptual unification that can be achieved by considering vibrational and relaxational processes in the same scheme, we devote a final section to this subject. Here we follow closely the development used in a recent review article.<sup>1a(ii)</sup>

In all the work reviewed so far, the frequency of the mechanical relaxation studies has not exceeded the 100-MHz range provided by ultrasonics. It is possible, though not easy, to make mechanical relaxation studies of glassy relaxations at extremely high frequencies in the gigahertz range by inelastic light scattering techniques. A visible light beam, for instance, will interact with the natural density (refractive index) fluctuations in the material to produce or annihilate acoustic phonons and yield a scattered beam, the Brillouin line, which gives information on the frequency, velocity, and damping of these phonons. The damping is reflected in the half-width of the Brillouin line. Such scattering techniques have been very valuable in the study of viscous liquids<sup>9,54,101-103</sup> and may be applied to the study of mechanical relaxation in fast-conducting solids if the strength of the associated relaxation is large enough. A couple of cases that satisfy this condition have recently been reported in the literature,<sup>38,104,105</sup> and we briefly summarize the value of such studies here.

The first case in question is the AgI-Ag<sub>2</sub>B<sub>4</sub>O<sub>7</sub> system in which there already existed extensive data at lower frequencies covering the range 1-110 Hz (by dynamic

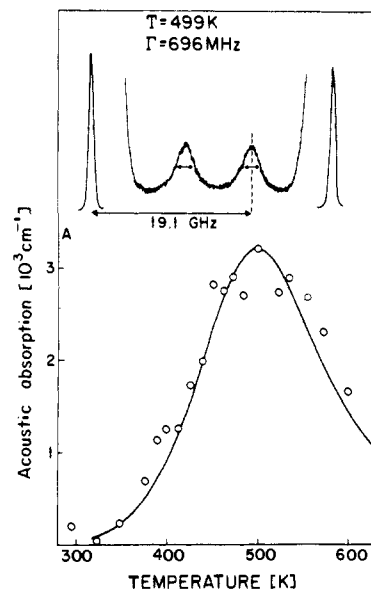


Figure 15. Brillouin spectra for 0.6AgI-0.4Ag<sub>2</sub>B<sub>4</sub>O<sub>7</sub> glass at 499 K, showing 19.1-GHz frequency shift from central exciting line and Brillouin half-width. Lower portion shows absorption coefficients at different temperatures obtained from Brillouin line widths of the upper portion.

mechanical studies discussed earlier;<sup>38</sup> see Figure 11) and by ultrasonic studies.<sup>105</sup> The relaxation in this glass is one that satisfies the two conditions, high relaxation strength and exceptionally short relaxation time at  $T_g$ , which are necessary for the observation of gigahertz phonon damping at temperatures below the glass transition temperature.

Figure 15 shows, in the upper portion, the basic experimental observation viz., the scattered Brillouin peak in relation to the central exciting line, and (in the lower portion) the important relaxation data in the form of absorption coefficients obtained at each temperature from the width of the Brillouin line. We see in Figure 11 how the absorption coefficient passes through a maximum at a temperature, 499 K, some 180 °C below the glass transition temperature for this system. Similar results have since been observed for a range of compositions in the same AgI-Ag<sub>2</sub>B<sub>4</sub>O<sub>7</sub> system<sup>104</sup> and also in the alkali halide containing system LiCl-LiB<sub>2</sub>O<sub>7</sub>.<sup>105</sup>

These data can be put in the reciprocal temperature form and displayed informatively with the results of the lower frequency experiments as shown in Figure 16.

Since the evidence from both electrical conductivity and low-frequency mechanical relaxation is that the activation energy for the mobile ion relaxation is mostly independent of temperature, we can assume (remembering the evidence in section V that, where studied, the spectral shape was constant with temperature) that the data displayed in Figure 16 reflect the spectral form of the relaxation as discussed using Figure 5. In this case, we may make the important observation from Figure 12 that the departure from exponential relaxation which is so pronounced at low temperatures is greatly reduced in the high-frequency short relaxation time range explored by the Brillouin scattering technique. Indeed the width of the relaxation in  $1/T$  can be accounted for almost quantitatively under the assumption of a single relaxation time. This appears also to be the case for the lithium cation motion in the LiCl-LiB<sub>2</sub>O<sub>7</sub> system<sup>105</sup> and hence is probably of general

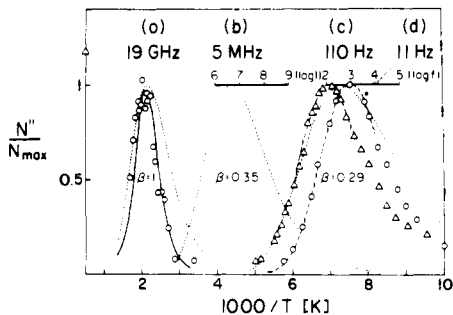


**Figure 16.** Comparison of normalized moduli for mechanical relaxation over wide temperature and frequency regimes using  $1/T$  representation of spectra form. Note that the spectra at 5 MHz (from ref 106) and 11 Hz are approximately the same in shape, while the high-temperature high-frequency spectrum is narrow. Dotted lines show predicted shapes at gigahertz and low frequencies according to the Gaussian activation energy distribution model of ref 106. The frequency scales attached to the 5-MHz and 110-Hz plots are based on the equivalence of  $1/T$  and  $\log f$  discussed earlier under Figure 4. Each scale has its origin fixed such that the peak of the modulus plot falls at the appropriate fixed frequency, 5 MHz or 110 Hz.

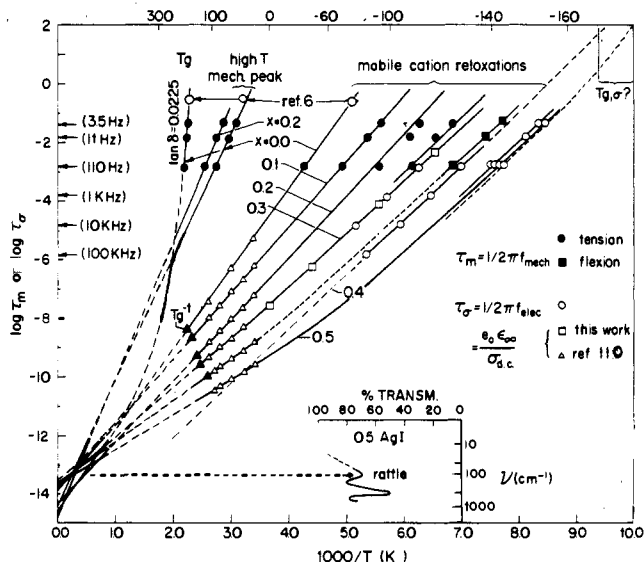


**Figure 17.** Relaxation "map" for mechanical and electrical relaxation in AgI-AgPO<sub>3</sub> glasses. High-temperature conductivity data from ref 110 have been converted to electrical relaxation times ( $\tau_e$ ), assuming a high-frequency dielectric constant of 15 for all cases. Conductivity and mechanical relaxation data are now available for the liquid states of this system but are omitted for clarity. Inset: Low-frequency portion of thin-film transmission IR spectra for 0.5 AgI-0.5AgPO<sub>3</sub> glass. Note coincidence of far-IR peaks (quasi-lattice vibration modes) with attempt frequency for relaxation modes. Reprinted from ref 50; copyright 1980 Elsevier Science Publishers B.V.

validity. An account of how the results of these studies can be accounted for within the coupling model has been given Ngai and Rendell.<sup>107</sup>

With this extended frequency/relaxation time data now in mind, it is helpful to make a summary representation of the variations of relaxation time with temperature that have been observed in different systems. Figure 17 shows a relaxation time map for the system AgI-AgPO<sub>3</sub><sup>50</sup> and includes some short longitudinal relaxation time data obtained by Brillouin scattering in the liquid state,<sup>54</sup> in addition to the various glassy-state data discussed in earlier papers. Figure 17 shows three important features, which we note again here.

First, it shows that for both electrical and mechanical relaxation the activation energy changes systematically

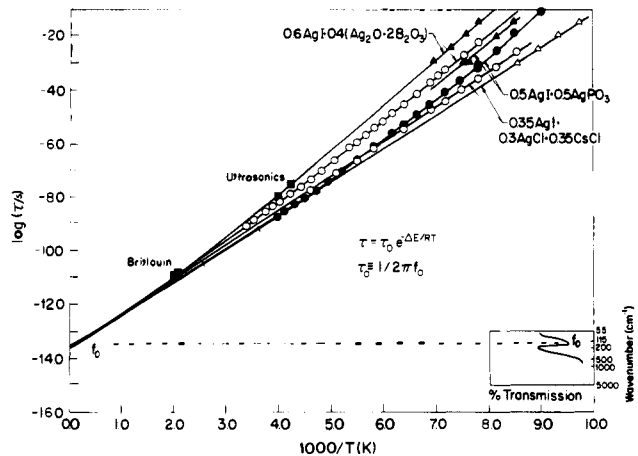


**Figure 18.** Arrhenius plot of relaxation times for mechanical and electrical mobile ion controlled processes in three different fast ion conducting glass systems, one containing only halide ions. Note that the latter, which has fully annealed, shows Arrhenius behavior over the whole temperature range with direct extrapolation to the quasi-lattice vibration time. Plot contains results of high-frequency study of Figures 15 and 16.<sup>104,105</sup>

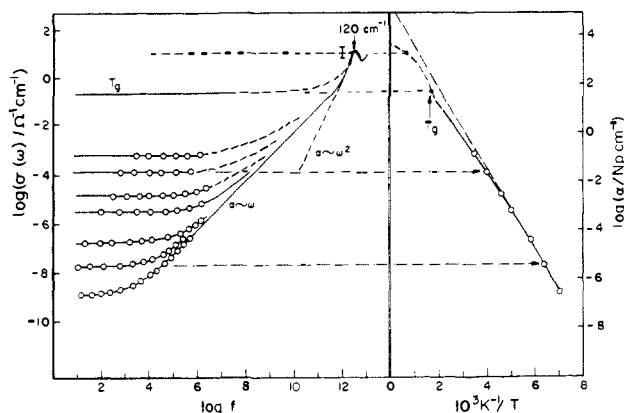
with composition in such a way that the slope of the least rapidly relaxing compositions tends toward the (much greater) slope of the viscoelastic relaxation.

Second, we note that (in contrast with other cases mentioned above, and included in Figures 13 and 14) the most rapidly relaxing compositions showed distinct departures from Arrhenius behavior in both electrical and mechanical relaxation. Whether or not this can be associated, as for viscous liquids, with measurable contributions to the thermodynamic properties (heat capacity, compressibility, etc.) from configurational degrees of freedom that are localized so as to be dissociated from the main viscoelastic relaxation, is not known at this time.

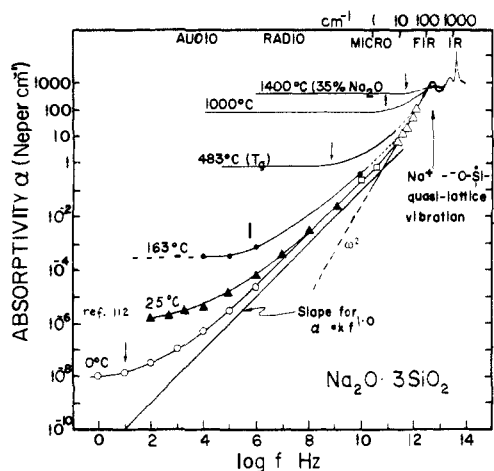
Third, all modes (including some secondary mechanical relaxation modes which are not associated with mobile cations and which we have not discussed) appear to be extrapolating toward a high-temperature limit which is broadly consistent with the "quasi-lattice" vibrational times observable by far-infrared spectroscopy on these systems.<sup>50,108</sup>

Figure 18 shows the relaxation times for the mobile ion modes alone for three different fast ion conducting systems and establishes that the very fast relaxing systems are not necessarily associated with departures from Arrhenius behavior. Indeed the one detailed study of this curvature in the literature, performed on the system AgI-Ag<sub>2</sub>MoO<sub>4</sub><sup>109</sup> suggests that it is a strong function of thermal treatment and indeed disappears after the glass has been properly annealed. We note here that a new study on AgI-AgPO<sub>3</sub> glasses by Malugani and Johari,<sup>110</sup> who used carefully annealed samples, has also found Arrhenius behavior at all compositions. This question deserves more detailed study.

Finally, we show in Figures 19 and 20 connections between relaxational and vibrational modes associated with electrical and mechanical fast ion relaxation. Figure 19 shows how the temperature dependence and the frequency dependence of the conductivity can be related to the absorption of energy from the oscillating electrical field, an absorption that reaches its maximum at frequencies in the far-infrared region of the electromagnetic spectrum, i.e., at frequencies characteristic of



**Figure 19.** Frequency dependence of electrical conductivity  $\sigma(\omega)$  (left-hand ordinate) and absorption coefficient  $\alpha_\omega$  (right-hand ordinate) due to fast ion motion at different temperatures for the fast ion conducting system  $0.6\text{AgI}\cdot 0.4(\text{Ag}_2\text{O}\cdot 2\text{B}_2\text{O}_3)$  (part a) and temperature dependence (Arrhenius plot) (part b), showing near equivalence of limiting high-frequency conductivity of the liquid state. Note changeover from a first-power frequency dependence of ac conductivity in most of the range to an  $\omega^2$  dependence near the quasi-lattice resonance absorption region.



**Figure 20.** Dependence of ac conductivity  $\sigma(f)$  and the related optical absorptivity  $\alpha$  on frequency for the case of  $\text{Na}_2\text{O}\cdot 3\text{SiO}_2$ , for which the most extensive data are available. Diagram shows connection of low-frequency dispersion region to infrared resonance absorption region via linear and quadratic dependence regimes for which fractal and anharmonic dynamics, respectively, are believed responsible.

the quasi-lattice vibrations. The (ac) conductivity at these frequencies is very high since every charged particle in the system is contributing in proportion to its charge as it vibrates at thermal velocities, creating an instantaneous fluctuating current. This conductivity can be measured by determining the loss of energy from a far-infrared light beam as the electromagnetic wave couples to the oscillating electric field and is absorbed.<sup>108</sup>

The relation is given by

$$\alpha(\omega) = \sigma(\omega)/e_0cn(\omega) \quad (12)$$

where  $e_0$  is the permittivity of free space,  $c$  is the velocity of light, and  $n(\omega)$  is the frequency-dependent refractive index, which, in a disordered transparent material, varies only weakly about the higher frequency value fixed by the electronic motions. Figure 19 has a conductivity scale on the right and the equivalent optical absorption coefficient scale on the left. Note how, as the temperature increases, the dc conductivity—

hence also the low-frequency absorption coefficient—rises toward a limit set by the absorption due to the vibrating ions in the quasi-lattice. The latter has been measured quite accurately for sodium borate glasses<sup>108</sup> but is less certain for the present case (see error bar in Figure 19) because the film thickness of the blown silver ion glass film was only crudely measured.<sup>111</sup> It would appear from Figure 19 to be a measure of the limiting high dc conductivity obtainable in an ionic system. There is need for more quantitative evaluation of far-IR absorptivities in relation to temperature and composition in order that the physical picture given in Figure 19 can be fully completed and confirmed.

Figure 19 gives the picture unifying vibrational and relaxational modes responding to electrical stresses. It shows how the absorption (per  $\text{cm}^{-1}$ ) by relaxational modes increases continuously with decreasing relaxation time, until they merge at the high-temperature, high-frequency extreme. The extrapolation between admittance bridge and far-IR absorption data in Figure 19 may seem unacceptably speculative. However, it may be justified by reference to systems for which the data are much more complete, thanks to recent gigahertz bridge measurements by Sridhar on  $\text{AgI}\text{-AgPO}_3$  glass<sup>112</sup> and time-domain reflectivity measurements by Burns, Cole, and Risen.<sup>113</sup> In Figure 20 we add data of the latter authors on  $\text{Na}_2\text{O}\cdot 3\text{SiO}_2$  to the original diagram from ref 1a(iii) to support the simple  $\sigma(\omega) \propto \omega^{1.0}$  connection we have suggested as the link between the low-temperature dc and high-frequency (infrared) ac conductivity regimes.

The origin of the implied constant loss, irrespective of wavelength (the existence of which has been suggested at various times in the past),<sup>35,100,114</sup> must be a matter of concern. Length scale independence is, of course, the hallmark of fractal systems and, although glasses are unquestionably Euclidean geometrical objects, there are strong theoretical indications,<sup>115</sup> supported by molecular dynamics simulations<sup>116</sup> and, to an extent, experiment,<sup>117</sup> to suggest that their *dynamics* may be fractal at least over some range. Kieffer and Angell, for instance, recently showed by simulations on stretch-ruptured vitreous  $\text{SiO}_2$ <sup>116</sup> that the  $\text{SiO}_2$  structure remains Euclidean until the point of spinodal rupture at  $\sim 70\%$  of normal density and then develops a self-similar porosity with a Hausdorff dimension that changes systematically with density. The same structure exhibited the features of fractal dynamics with a fracton dimension falling a constant interval below the Hausdorff dimension except in the prerupture regime. In the latter regime, where the Hausdorff dimension was 3.0, the fracton dimension continued to change. However, it remained less than 3.0 at normal density, in accord with the Alexander-Orbach theory.<sup>114</sup>

If fractal dynamics are involved in the frequency-independent loss in glassy systems, then it should not be only electrical absorptivities that reveal them. We therefore turn to the results of ultrasonic and hypersonic studies to see whether similar behavior is manifested. Certainly it is known that the absorptivity in ultrasonic studies increases very rapidly with increasing frequency, and this usually sets the high-frequency limit on ultrasonic measurements.

For our example we choose the superionic glass  $3\text{AgI}\cdot 2\text{Ag}_2\text{B}_4\text{O}_7$  on which both high-quality ultrasonic



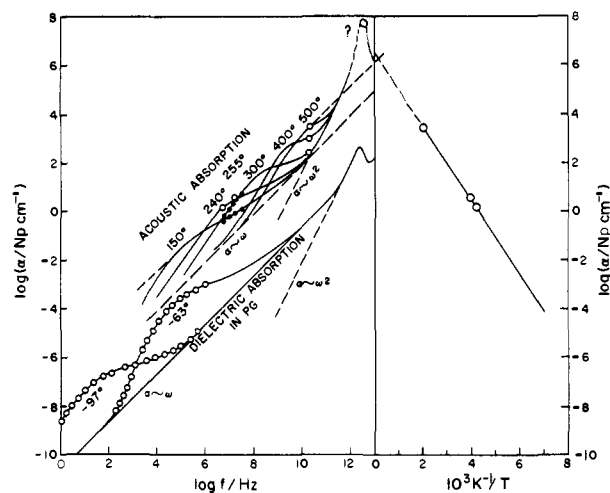


**Figure 21.** Analogue of Figure 19 for absorption of *mechanical* energy in the same system, based on limited ultrasonic<sup>11</sup> and Brillouin scattering<sup>31</sup> data. For comparison, data for absorption of electromagnetic waves by a relaxing dipolar fluid, propanediol,<sup>47</sup> over the same frequency range are included. Both seem to have similar  $\alpha \sim f^{1.0}$  backgrounds over the major part of the frequency range. An Arrhenius temperature dependence for the acoustic absorption coefficient (at the frequency of the loss maximum) is a novel observation to the best of our knowledge.

data<sup>106</sup> and hypersonic data<sup>38,104</sup> exist. Figure 15, for example, shows that peak absorption in the gigahertz range is  $3.1 \times 10^3$  Np m<sup>-1</sup> at 499 K. The data are plotted in Figure 21 along with additional data discussed below.

Since the mechanical relaxation is one which leads to a thermodynamic state of polarization, we cannot expect the equivalent of Figure 19 for mechanical motions to have the frequency-independent plateaus of Figure 19 (though this would be the case for shear relaxation in liquids). Rather, the nearest equivalent would be the relaxation of a polar liquid. Data connecting dielectric relaxation and IR absorption were recently published for the case of propanediol<sup>118</sup> and are reproduced in Figure 21 (part a lower curves) to provide a basis for comparison with the mechanical analogue which we now discuss.

The peak absorption data from ultrasonic studies are entered in Figure 21 as functions of frequency in part a and of reciprocal temperature in part b, as in Figure 19. A few off-peak absorptivities at different ultrasonic frequencies allow us to estimate the form of the acoustic absorption shoulders at different temperatures. We do not have the equivalent of a far-infrared absorption coefficient for the mechanical modes, but we do know that longitudinal acoustic excitations with the normal velocity of sound are observable in some glasses by neutron scattering in the equivalent of the second Brillouin zone at wave vectors for which the wavelength is of the order of 10 Å.<sup>119</sup> Furthermore, these excitations<sup>120</sup> are not observable at lower wave vectors in liquid or glassy states, which implies overdamping. Therefore, we can write, for the smallest physically meaningful wavelength  $\lambda_{\min}$ , which is the interatomic spacing

$$\alpha \lambda_{\min} \geq 1 \quad (13)$$

which implies that the wave is completely damped in a single wavelength. Furthermore, this limiting high absorption coefficient will occur at a frequency given by

$$\lambda_{\min} f_{\max} = V \quad (14)$$

where  $v$  is the velocity of sound. Substituting  $v = 2 \times 10^5$  cm s<sup>-1</sup>(<sup>106</sup>) and  $\lambda_{\min} = 2 \times 10^{-8}$  cm we find from eqs 13 and 14 that  $\alpha_{\max} = 5 \times 10^7$  cm<sup>-1</sup> at  $f = 1 \times 10^{13}$  Hz. This, however, must be an underestimate because the sound velocity at such short wavelengths must be much smaller than the normal value. Entering this value in Figure 21 and making the most natural connections to the isothermal curves passing through lower frequency points, we recover a pattern quite similar to that for dielectric relaxation. The main difference is a more prominent peak absorption. This is due partly to the greater broadness of the mechanical relaxation, which diminishes the maximum absorptivity of the lower frequency peaks. Some difference might also be expected from the different physics involved in the respective highest frequency peaks. By different physics we mean that the wavelength of the excitation being damped at the mechanical absorption peak is quite different from that of the optical mode that is being excited at the center of the glassy-state equivalent of the crystalline-state Brillouin zone. The latter is strongly, but not completely, absorbed.

We find it of interest that, despite the different physics, there should be as much similarity as there is in the two cases. In particular, the apparent presence of a mechanical equivalent of the source of constant loss per unit wavelength at frequencies well above the relaxation peak is encouraging. This implies a common origin and would be consistent with our speculation that fracton modes may be involved as a common explanation. Indeed, a crossover from phonon to fracton dynamics in lithium borate glasses has recently been suggested by Borjesson<sup>121</sup> to explain particular light-scattering observations. We note again the evidence for a constant  $1/T_1$ , which is equivalent to a constant loss in modulus spectroscopy, in the studies of low-temperature Li NMR spectroscopy,<sup>71,79</sup> so the phenomenon is common to all of the dynamic probes we have considered in this article.

From study of a variety of systems, it would appear that the magnitude of the constant background loss can vary greatly from system to system and may be sensitive to thermal annealing. We have observed<sup>121</sup> more than two-decade variations from system to system with no particular pattern or correlation with glass composition or liquid class so far emerging. It would seem to present a substantial challenge to future experimental and theoretical endeavor.

## IX. Omissions

I am well aware of, and concerned about, the fact that this review is incomplete. Most obvious by its absence is any analysis of the many current theoretical interpretations of different aspects of the phenomenology we have described. However, even some significant aspects of the phenomenology—e.g., the effect of the pressure variable—have not been dealt with, and the studies by computer simulation largely from laboratory have been omitted completely. These must await future reviews.

For the moment, we compromise by only noting the existence of new or alternative theoretical accounts (in addition to those mentioned in the earlier text) of the

origin of nonexponential relaxation in conducting solids by Funke,<sup>123</sup> Shlesinger,<sup>74</sup> Schirmacher,<sup>124</sup> and Dyre<sup>125</sup> and a new treatment of the motion of ions over or through a fluctuating energy barrier by Stein et al.<sup>126</sup> Recent simulation results can be seen in refs 127–129.

I extend an apology to all authors whose significant contributions to this interesting subject area have been inadequately dealt with and exhort future reviewers of this area to excel where I have faltered.

## X. Conclusions

Decoupled ion motions in glassy solids lead to a rich variety of relaxation phenomena. Comparison of electrically, mechanically, and magnetically stimulated relaxation phenomena reveals considerable common character, particularly with respect to the relaxation function. This is mostly, though not universally, of stretched exponential (fractal time, or KWW) form, though the departure from exponentiality varies from probe to probe; mechanical relaxation tends to be less exponential, while NMR and conductivity relaxations have very similar functions.

On the basis of the more widely available electrical relaxation data, we establish a linear correlation between the nonexponentiality parameter,  $\beta$  of the KWW function, and the decoupling index  $R_{\infty}$ , which quantifies the independence of fast-ion modes from viscosity modes: the more decoupled the conductivity, the more nonexponential the relaxation.

Finally, we observe, in all relaxations, evidence for a constant frequency-independent loss between resonance and relaxation frequency domains which we speculate may be connected to fracton dynamics endemic to the glassy state.

## XI. Acknowledgments

I acknowledge very helpful discussions with R. W. Rendell and G. P. Johari. This work has benefited from the financial support of the Department of Energy under Grant No. DE-F602-89ER45398 and the Office of Naval Research under Agreement No. N00014-84-K-0289.

## XII. References

- (1) (a) Relaxation and relaxation spectroscopy in glasses and viscous liquids: (i) Lamb, J. *Rheol. Acta* 1973, 12, 438; (ii) Brawer, S. A. *Relaxation in Viscous Liquids*; American Ceramic Society: Columbus, OH, 1985; (iii) Wong, J.; Angell, C. A. *Glass: Structure by Spectroscopy*; Marcel Dekker: New York, 1976; Chapter 13; (iv) Angell, C. A. *Mater. Chem. Phys.* 1989, 23, 143. (b) Nonexponential relaxation in condensed matter: (i) Ngai, K. In *Non-Debye Relaxation in Condensed Matter*; Ramakrishnan, T. V., Raj Lakshmi, M., Eds.; World Scientific: Singapore, 1987; p 23; (ii) Stein, D. L.; Palmer, R. G. *Glasses I: Phenomenology* (includes a brief review of theoretical models). In *Lectures in the Sciences of Complexity*; Stein, D. C., Ed.; Addison-Wesley: New York, 1989; (iii) Shlesinger, M. F. *Annu. Rev. Phys. Chem.* 1988, 39, 269. (c) Fast ion motion in glasses: (i) Souquet, J.-L. *Solid State Ionics* 1981, 5; *Annu. Rev. Mater. Sci.* 1981, 11, 211; (ii) Tuller, H. L.; Button, D. P.; Uhlmann, D. R. *J. Non-Cryst. Solids* 1983, 40, 93; (iii) Minami, T. *J. Non-Cryst. Solids* 1985, 73, 273; (iv) Angell, C. A. *Solid State Ionics* 1983, 9 & 10, 3; 1986, 18 & 19, 72. (v) Ingram, M. D. *J. Non-Cryst. Solids* 1985, 73, 247. (d) Nuclear magnetic resonance studies of ionic motion in glasses: (i) Bray, P. J.; Geissburger, A. E.; Buchaltz, F.; Harris, I. A. *J. Non-Cryst. Solids* 1982, 52, 45; (ii) Müller-Warmuth, W.; Eckert, H. *Phys. Rep.* 1982, 88, 91; (iii) Martin, S. W. *Mater. Chem. Phys.* 1989, 23, 225. (e) Mechanical and dielectric relaxation in polymeric solids: (i) McCrum, M. G.; Reid, B. E.; Williams, G. *Anelastic and Dielectric Effects in Polymeric Solids*; Wiley: London, New York, 1967. (f) Low-temperature phenomena: hole-burning relaxation studies: (i) Hayes, J. M.; Jankowiak, R.; Small, G. J. In *Topics in Current Physics. Persistent Spectral Hole Burning: Science and Applications*. Moerner, W. E., Ed.; Springer-Verlag: New York, 1988.
- (2) (a) Turnbull, D. *Contemp. Phys.* 1969, 10, 473. (b) Turnbull, D.; Cohen, M. H. *J. Chem. Phys.* 1970, 52, 3038.
- (3) Dubochet, J.; Adrian, M.; Teixeira, J.; Alba, C. M.; Kadiyala, R. D.; MacFarlane, D. R.; Angell, C. A. *J. Phys. Chem.* 1984, 88, 6727.
- (4) Hilderbrand, E. A.; McKinnon, I. R.; MacFarlane, D. R. *J. Chem. Phys.* 1986, 90, 2784.
- (5) See, for instance: *Dynamic Aspects of Structural Change in Liquids and Glasses*; Angell, C. A., Goldstein, M., Eds.; Ann. N.Y. Acad. Sci. 484; New York Academy of Sciences: New York, 1986. Also see reviews by: (a) Wolynes, P. G. In *Proceedings of the International Symposium on Frontiers in Science*; Chan, S. S., Debrunner, P. G., Eds.; AIP Conf. Proc. 180, 1988. (b) Jackle, J. *Rep. Prog. Phys.* 1986, 49, 171.
- (6) Angell, C. A.; Clarke, J. H. R.; Woodcock, L. V. *Adv. Chem. Phys.* 1981, 48, 397.
- (7) Brawer, S. A. *Relaxation in Viscous Liquids*; American Ceramic Society: Columbus, OH, 1985.
- (8) Torell, L. M.; Angell, C. A. *J. Chem. Phys.* 1983, 78, 937.
- (9) Angell, C. A. In *Relaxations in Complex Systems*; Ngai, K., Wright, G. B., Eds.; National Technical Information Service, U.S. Department of Commerce: Springfield, VA, 1985; p 1. The descriptions "strong" and "fragile" for liquids, while now frequently seen in the literature, are a recent arrival and may not be familiar to the reader. In essence they refer to behavior associated with the degree of departure of liquid viscosity from the Arrhenius law. Large departures over wide temperature ranges, implying very large activation energies near  $T_g$ , signal "fragile" behavior (examples: toluene, o-terphenyl,  $\text{KNO}_3$ - $\text{Ca}(\text{NO}_3)_2$  melts). Strong liquids conform to the Arrhenius law over the whole liquid range down to  $T_g$  (example:  $\text{SiO}_2$ ).
- (10) Angell, C. A. *Ann. Y.Y. Acad. Sci.* 1981, 371, 136.
- (11) Goldstein, M. *J. Chem. Phys.* 1969, 51, 3728.
- (12) Johari, G. P.; Goldstein, M. *J. Chem. Phys.* 1970, 53, 2372; 1971, 55, 4245.
- (13) Johari, G. P. (a) *J. Phys. Colloq.* 1985, 46 (C8), 567. (b) In *Relaxation in Complex Systems*; Ngai, K., Wright, G. B., Eds.; National Technical Information Service, U.S. Department of Commerce: Springfield VA, 1984; p 17.
- (14) Fischer, E. W.; Hellman, G. P.; Spiess, H. W.; Horth, F. J.; Ecarius, U.; Wehrle, M. *Macromol. Chem. Phys.* 1985, Suppl. No. 12, 189.
- (15) Johari, G. P. *J. Chem. Phys.* 1973, 58, 1755; *Polymer* 1986, 27, 566.
- (16) Many examples for polymer glasses have been described and analyzed: (a) McCrum, M. G.; Reid, B. E.; Williams, G. *Anelastic and Dielectric Effects in Polymeric Solids*; Wiley: London, New York, 1967. (b) Ngai, K. In *Non-Debye Relaxation in Condensed Matter*; Ramakrishnan, T. V., Raj Lakshmi, M., Eds.; World Scientific: Singapore, 1987; p 23. (c) Ngai, K. L.; Rendell, R. W.; Rajagopal, A. K.; Teitler, S. *Ann. N.Y. Acad. Sci.* 1986, 484, 150. (d) Ngai, K. *Solid State Ionics* 1987, 5, 27.
- (17) Geszti, T. *J. Phys. C: Solid State Phys.* 1980, 101A, 477.
- (18) Leutheusser, E. *Phys. Rev.* 1984, A29, 2765. (b) Bengtzelius, V.; Göeze, W.; Sjölander, A. *J. Phys. C: Solid State Phys.* 1984, 17, 5915.
- (19) (a) Das, S. P.; Mazenko, G. F. *Phys. Rev.* 1986, A34, 2265. Das, S. P. *Phys. Rev.* 1987, A36, 211. (b) Götze, W.; Sjögren, L. *Z. Phys.* 1987, B65, 415.
- (20) Goetze, W. In *Liquids, Freezing, and the Glass Transition*; Hansen, J.-P., Levesque, D., Eds.; NATO-ASI Series; Plenum: New York, in press.
- (21) Spaepen, F. *Ann. N.Y. Acad. Sci.* 1981, 371, 218.
- (22) McLin, M.; Angell, C. A. *J. Phys. Chem.* 1988, 92, 2083.
- (23) Macedo, P. B.; Moynihan, C. T.; Bose, R. *Phys. Chem. Glasses* 1972, 13, 171.
- (24) (a) Howell, F. S.; Bose, R. A.; Macedo, P. B.; Moynihan, C. T. *J. Phys. Chem.* 1974, 78, 639. (b) Moynihan, C. T.; Balytactac, N.; Boone, L.; Litovitz, T. A. *J. Chem. Phys.* 1971, 55, 3013.
- (25) Angell, C. A. (a) *Solid State Ionics* 1983, 9/10, 3; (b) 1986, 18/19, 72.
- (26) Souquet, J. L. *Annu. Rev. Mater. Sci.* 1981, 11, 211.
- (27) Borjesson, L.; Stevens, J. R.; Torell, L. M. *Polymer* 1987, 28, 1803.
- (28) Etienne, S.; Cavaille, Y.; Perez, J.; Johari, G. P. *Philos. Mag.* 1985, 51, L35.
- (29) Johari, G. P.; Pathmanathan, K. *Phys. Chem. Glasses* 1988, 29, 219.
- (30) Cavaille, J. Y.; Perez, J.; Johari, G. P. *Phys. Rev. B* 1989, 39, 2411.

- (31) Törmälä, P. J. *Macromol. Sci., Rev. Macromol. Chem.* 17, 297; 28, 2567.
- (32) Hakim, R. M.; Uhlmann, D. R. *Phys. Chem. Glasses* 1971, 12, 132.
- (33) Wong, J.; Angell, C. A. *Glass: Structure by Spectroscopy*; Marcel Dekker: New York, 1976; Chapter 11.
- (34) Provenzano, V.; Boesch, L. P.; Volterra, V.; Moynihan, C. T.; Macedo, P. B. *J. Am. Ceram. Soc.* 1972, 55, 494.
- (35) Moynihan, C. T.; Boesch, L. P.; Laberge, N. L. *Phys. Chem. Glasses* 1973, 14, 122.
- (36) Simmons, K.; Simmons, J. J. *Am. Ceram. Soc.* 1979, 62, 479.
- (37) Mangion, M. B. M.; Johari, G. P. *Phys. Chem. Glasses* 1988, 29, 225; 1989, 30, 180.
- (38) Borjesson, L.; Torell, L. M.; Martin, S. W.; Changle Liu; Angell, C. A. *Phys. Lett.* 1987, 125, 330.
- (39) Weiler, R.; Bose, R.; Macedo, P. B. *J. Chem. Phys.* 1970, 53, 1258.
- (40) (a) Torell, L. M. *J. Chem. Phys.* 1982, 76, 3467. (b) Torell, L. M.; Angell, C. A. *J. Chem. Phys.* 1983, 78, 937.
- (41) Sidebottom, D.; Sorenson, C. *Phys. Rev. B* 1990, in press. We note that the recent impulsive light scattering study by Cheng et al. (Cheng, L.-T.; Yan, Y.-Z.; Nelson, K. A. *J. Chem. Phys.* 1989, 91, 6052) yields data in qualitative agreement, but significant quantitative disagreement, with the data of Figure 8.
- (42) Hodge, I. M.; Angell, C. A. *J. Chem. Phys.* 1977, 67, 4.
- (43) Torell, L. M.; Ziegler, D. C.; Angell, C. A. *J. Chem. Phys.* 1984, 81, 5053.
- (44) Dixon, P.; Nagel, S. *Phys. Rev. Lett.* 1988, 61, 341 and private communication.
- (45) (a) Tomazawa, M. In *Treatise on Materials Science*; Tomazawa, M., Doremus, R. H., Eds.; Academic: New York, 1977; Vol. XII, p 335. (b) Hyde, J. M.; Tomazawa, M. *J. Non-Cryst. Solids* 1989, 109, 18. (c) McGahay, V.; Tomazawa, M. *J. Non-Cryst. Solids* 1989, 109, 27.
- (46) Boesch, L. P.; Moynihan, C. T. *J. Non-Cryst. Solids* 1975, 17, 144.
- (47) Day, D. E.; Stevels, J. M. *J. Non-Cryst. Solids* 1973, 13, 304.
- (48) Etienne, S.; Cavaille, J. Y.; Perex, J.; Point, R.; Salvia, M. *Rev. Sci. Instrum.* 1982, 53, 126.
- (49) Mai, C.; Assiero, A.; Johari, G. P.; Etienne, S.; Abbes, K. J. *Non-Cryst. Solids* 1987, 93, 35.
- (50) (a) Atake, T.; Angell, C. A. *J. Non-Cryst. Solids* 1980, 39/39, 439. (b) Liu, C.; Angell, C. A. *J. Non-Cryst. Solids* 1986, 83, 162.
- (51) Copley, G. J.; Oakley, D. R. *Phys. Chem. Glasses* 1968, 9, 141.
- (52) Dixon, P. K.; Nagel, S. R. *Phys. Rev. Lett.* 1988, 61, 341, communication.
- (53) (a) Chiodelli, A.; Magistris, A. *Mater. Res. Bull.* 1982, 17, 1.
- (54) (a) Torell, L. M. *Phys. Rev.* 1985, B31, 4103. (b) Borjesson, L.; Martin, S. W.; Torell, L. M.; Angell, C. A. *Solid State Ionics* 1986, 18/19, 141.
- (55) Susman, S.; Boehm, L.; Volin, H. J.; Delbecq, C. T. *Solid State Ionics* 1981, 5, 667.
- (56) Carette, B.; Ribes, M.; Souquet, J. L. *Solid State Ionics* 1985, 9/10, 735.
- (57) Pradel, A.; Ribes, M.; Maurin, M., to be published in *Solid State Ionics*.
- (58) Robinel, E.; Carette, B.; Ribes, M. *J. Non-Cryst. Solids*, 1983, 57, 49.
- (59) Kennedy, J. H.; Yang, Y. J. *Solid State Chem.* 1987, 69, 252.
- (60) Kennedy, J. H.; Zhang, Z. *Solid State Ionics* 1988, 28/30, 726.
- (61) Minami, T.; Machida, N. *Mater. Chem. Phys.* 1989, 23, 63.
- (62) Doremus, R. H. *Glass Science*; Wiley: New York, 1973.
- (63) Day, D. E. In *Amorphous Solids*; Douglas, R. W., Ellis, B., Eds.; Wiley: London, 1972; p 39.
- (64) Moore, D. W.; Day, D. E. *Phys. Chem. Glasses*, 1971, 12, 75.
- (65) Ingram, M. D.; Moynihan, C. T. *Phys. Chem. Glasses* 1985, 26, 132.
- (66) Kulkarni, A. R., unpublished work.
- (67) Kulkarni, A. R.; Angell, C. A. *J. Non-Cryst. Solids* 1988, 99, 195.
- (68) Bloembergen, N.; Purcell, E. M.; Pound, R. V. *Phys. Rev.* 1978, 73, 679.
- (69) Bray, P. J.; Geissburger, A. E.; Buchaltz, F.; Harris, I. A. *J. Non-Cryst. Solids* 1982, 52, 45.
- (70) Müller-Warmuth, H.; Eckert, H. *Phys. Rep.* 1982, 88, 91.
- (71) Göbel, E.; Müller-Warmuth, W.; Olyschlöger, H. *J. Magn. Reson.* 1979, 36, 371.
- (72) Pradel, A.; Ribes, M. *Mater. Chem. Phys.* 1989, 23, 121.
- (73) (a) Ngai, K., In *Fast Ion Transport in Solids*; Vashishta, P., Mundy, J. N., Shenoy, G. K. Eds.; North-Holland: New York, 1979; p 203. (b) *Solid State Ionics* 1981, 5, 27. (These references actually addressed similar phenomena in non-vitreous disordered materials.)
- (74) Shlesinger, M. F. *Annu. Rev. Phys. Chem.* 1988, 39, 269.
- (75) (a) Martin, S. W. *Mater. Chem. Phys.* 1989, 23, 225. (b) *Appl. Phys. A* (Special edition), in press.
- (76) Angell, C. A. In *Phenomenology of fast ion conducting glasses: Facts and confusions*. *Solid Electrolytes*; Takahashi, T., Ed.; World Scientific Press: Singapore, 1989; p 89.
- (77) Angell, C. A.; Martin, S. W. *Symp. Mater. Res. Soc.* 1989, 135, 63.
- (78) Martin, S. W.; Bischof, H. J.; Mali, M.; Roos, J.; Brinkman, D. *Solid State Ionics* 1986, 18/19, 421.
- (79) (a) Reinecke, T. L.; Ngai, K. L. *Phys. Rev.* 1975, B12, 3476. (b) Seftel, J.; Alloul, H. *J. Non-Cryst. Solids* 1978, 29, 253. (c) Greenbaum, S. G.; Strom, U.; Rubinstein, M. *Phys. Rev.* 1982, B26, 5226. (d) Sisco, S. J.; Spellane, P.; Kennedy, J. H. *J. Electrochem. Soc.* 1985, 132, 1766. (e) Balzer-Jollenbeck, G.; Kanert, O.; Steinert, J.; Jain, H. *Solid State Commun.* 1988, 65, 3.
- (80) (a) Balzer-Jollenbeck, G.; Kanert, O.; Jain, H.; Ngai, K. L. *Phys. Rev. B* 1989, 39, 6071. (b) Ngai, K. L.; Martin, S. W. *Phys. Rev. B* 1989, 40, 10550.
- (81) Rendell, R. W.; Ngai, K. L.; Fong, G. R.; Aklonis, J. J. *Macromolecules* 1987, 20, 1070.
- (82) Angell, C. A. *J. Chem. Phys.* 1967, 46, 4673.
- (83) Angell, C. A.; Moynihan, C. T. In *Molten Salts: Characterization and Analysis*; Mamantov, G., Ed.; Marcel Dekker: New York, 1969; p 315.
- (84) Kauzmann, W. *Chem. Rev.* 1948, 46, 219.
- (85) Adam, G.; Gibbs, J. H. *J. Chem. Phys.* 1965, 43, 139.
- (86) (a) Kawamura, J.; Shimoji, M. *J. Non-Cryst. Solids* 1986, 88, 295. Kawamura, J.; Shimoji, M. *Mater. Chem. Phys.* 1989, 23, 99.
- (87) (a) Bose, B.; Weiler, R.; Macedo, P. B. *Phys. Chem. Glasses* 1970, 11, 117. (b) Tweer, H.; Laberge, N.; Macedo, P. B. *J. Am. Ceram. Soc.* 1971, 54, 121.
- (88) (a) Angell, C. A. *J. Phys. Chem. Solids* 1988, 49(8), 863. (b) *J. Non-Cryst. Solids* 1988, 102, 205.
- (89) Martin, S. W.; Angell, C. A. *J. Non-Cryst. Solids* 1986, 83, 185.
- (90) Liu, C.; Angell, C. A. *J. Chem. Phys.*, in press.
- (91) Rao, K. J.; Rao, C. N. R. *Mater. Res. Bull.* 1982, 17, 1337.
- (92) Goodman, C. H. L. *Phys. Chem. Glasses* 1985, 26, 1.
- (93) (a) Ingram, M. D. *Mater. Chem. Phys.* 1989, 23, 51; *Philos. Mag.* 1989, 60, 0000. (b) Ingram, M. D.; MacKenzie, M. A.; Müller, W.; Torge, M. *Solid State Ionics*, in press.
- (94) See, for instance: Mercier R.; Tachez, M.; Malugani, J. P.; Rousselet, C. *Mater. Chem. Phys.* 1989, 23, 13. Maugion, M.; Johari, G. P. *Phys. Rev. B* 1987, 36, 8845.
- (95) Jun, L.; Portier, J.; Tanguy, B.; Videau, J.-J.; Angell, C. A. *Solid State Ionics*, in press.
- (96) Lesikar, A. V.; Simmons, C. J.; Moynihan, C. T. *J. Non-Cryst. Solids* 1980, 40, 9171.
- (97) Rendell, R. W.; Ngai, K. L.; Fong, G. R.; Aklonis, J. J. *Macromolecules* 1987, 20, 1070.
- (98) (a) Downing, H. L.; Peterson, N. L.; Jain, H. *J. Non-Cryst. Solids* 1982, 50, 203. (b) Jain, H.; Petersen, N. L. *Philos. Mag.* 1982, A46, 351.
- (99) Ngai, K. L.; Rendell, R. W.; Jain, H. *Phys. Rev. B* 1984, 30, 2133.
- (100) Tatsumisago, M.; Hamada, A.; Minami, T.; Tanaka, M. *J. Non-Cryst. Solids* 1983, 56, 423; *J. Am. Ceram. Soc.* 1983, 66, 890.
- (101) Pinnow, D. A.; Candace, S. J.; LaMacchia, J. T.; Litovitz, T. A. *J. Account. Soc. Am.* 1968, 43, 131.
- (102) Higashigaki, Y.; Wang, C. H. *J. Chem. Phys.* 1981, 74, 3175.
- (103) Patterson, G. *Annu. Rev. Phys. Chem.* 1987, 38, 191.
- (104) Borjesson, L. *Phys. Rev.* 1987, B36, 4600.
- (105) Borjesson, L.; Torell, L. M. *Solid State Ionics* 1987, 25, 85.
- (106) Carini, G.; Cutroni, M.; Federico, M.; Galli, G.; Tripodo, G. *Phys. Rev.* 1984, B30, 7219; 1985, B32, 8264.
- (107) Ngai, K. L.; Rendell, R. W. *Phys. Rev. B* 1988, B38, 9987.
- (108) Liu, C.; Angell, C. A. *J. Chem. Phys.*, in press.
- (109) Ingram, M. D.; Vincent, C. A.; Wandless, A. R. *J. Non-Cryst. Solids* 1982, 53, 73.
- (110) Malugani, J. P.; Wasniesnski, A.; Dorean, M.; Robert, G.; Al Rikabi, A. *Mater. Res. Bull.* 1978, 13, 427.
- (111) Liu, Changle, unpublished work.
- (112) Sridhar, S., to be published.
- (113) Burns, A. V.; Cole, R. H.; Chrysachos, G.; Risen, W. *Phys. Chem. Glasses* 1989, 30, 264.
- (114) Ngai, K. L.; Strom, V. *Phys. Rev. B* 1983, B27, 603.
- (115) Alexander, S.; Orbach, R. *J. Phys. Lett.* 1982, 43, L-625.
- (116) Kieffer, J. A.; Angell, C. A. *J. Non-Cryst. Solids* 1988, 106, 336.
- (117) Khonneux, P.; Courtens, E.; Pelous, J.; Vacher, R. *Europhys. Lett.* 1989, 10, 733.
- (118) Boehm, L.; Smith, D. L.; Angell, C. A. *J. Mol. Liquids* 1987, 36, 153.
- (119) Leadbetter, A. J.; Wright, A. C.; Apling, A. J. In *Amorphous Materials*; Douglas, R. W., Ellis, B., Eds.; Wiley-Interscience: London, 1972.
- (120) Grest, G. S.; Nagel, S. R.; Rahman, A. *Phys. Rev. B* 1984, B29, 5968.
- (121) Borjesson, L. In *Dynamics of Disordered Materials*; Richter, D., Dianoux, A. J., Petry, W., Teixeira, J., Eds.; Springer-Verlag: Berlin, 1989; Vol. 37, p 126.

- (122) Angell, C. A. Unpublished work.
- (123) Funke, K.; Hoppe, R. *Solid State Ionics* 1986, 18-19, 183; 1988, 28-30, 100; 1990, in press.
- (124) Movaghar, B.; Schirmacher, W. *J. Phys.* 1981, C14, 859.
- (125) Dyre, J. C. *J. Appl. Phys.* 1988, 64, 2456 and earlier references therein.
- (126) Stein, D. L.; Palmer, R. G.; Van Hemmen, J. L.; Doering, C. R. *Phys. Lett.* 1989, 136, 353.
- (127) Angell, C. A.; Boehm, L.; Cheeseman, P. A.; Tamaddon, S. *Solid State Ionics* 1981, 5, 659.
- (128) Angell, C. A.; Cheeseman, P. A.; Tamaddon, S. *J. Phys. Colloq.* 1982, 43, C9-381.
- (129) Syed, R.; Kieffer, J. A.; Angell, C. A. *Symp. Mater. Res. Soc.* 1989, 135, 73.